







TECH BRIEFS

NATIONAL AERONAUTICS AND SPACE ADMINISTRATION

-  **Technology Focus**
-  **Computers/Electronics**
-  **Software**
-  **Materials**
-  **Mechanics**
-  **Machinery/Automation**
-  **Manufacturing**
-  **Bio-Medical**
-  **Physical Sciences**
-  **Information Sciences**
-  **Books and Reports**

INTRODUCTION

Tech Briefs are short announcements of innovations originating from research and development activities of the National Aeronautics and Space Administration. They emphasize information considered likely to be transferable across industrial, regional, or disciplinary lines and are issued to encourage commercial application.

Availability of NASA Tech Briefs and TSPs

Requests for individual Tech Briefs or for Technical Support Packages (TSPs) announced herein should be addressed to

National Technology Transfer Center

Telephone No. (800) 678-6882 or via World Wide Web at www2.nttc.edu/leads/

Please reference the control numbers appearing at the end of each Tech Brief. Information on NASA's Commercial Technology Team, its documents, and services is also available at the same facility or on the World Wide Web at www.nctn.hq.nasa.gov.

Commercial Technology Offices and Patent Counsels are located at NASA field centers to provide technology-transfer access to industrial users. Inquiries can be made by contacting NASA field centers and program offices listed below.

NASA Field Centers and Program Offices

Ames Research Center

Lisa L. Lockyer
(650) 604-3009
lisa.l.lockyer@nasa.gov

Dryden Flight Research Center

Gregory Poteat
(661) 276-3872
greg.poteat@dfrc.nasa.gov

Goddard Space Flight Center

Nona Cheeks
(301) 286-5810
Nona.K.Cheeks.1@gpsc.nasa.gov

Jet Propulsion Laboratory

Ken Wolfenbarger
(818) 354-3821
james.k.wolfenbarger@jpl.nasa.gov

Johnson Space Center

Charlene E. Gilbert
(281) 483-3809
commercialization@jsc.nasa.gov

Kennedy Space Center

Jim Aliberti
(321) 867-6224
Jim.Aliberti-1@ksc.nasa.gov

Langley Research Center

Jesse Midgett
(757) 864-3936
jesse.c.midgett@nasa.gov

John H. Glenn Research Center at Lewis Field

Larry Viterna
(216) 433-3484
cto@grc.nasa.gov

Marshall Space Flight Center

Vernotto McMillan
(256) 544-2615
vernotto.mcmillan@msfc.nasa.gov

Stennis Space Center

Robert Bruce
(228) 688-1929
robert.c.bruce@nasa.gov

NASA Program Offices

At NASA Headquarters there are seven major program offices that develop and oversee technology projects of potential interest to industry:

Carl Ray

Small Business Innovation Research Program (SBIR) & Small Business Technology Transfer Program (STTR)
(202) 358-4652 or
cray@nasa.gov

Benjamin Neumann

Innovative Technology Transfer Partnerships (Code TD)
(202) 358-2320
benjamin.j.neumann@nasa.gov

John Mankins

Office of Space Flight (Code TD)
(202) 358-4659 or
john.c.mankins@nasa.gov

Terry Hertz

Office of Aero-Space Technology (Code RS)
(202) 358-4636 or
thertz@nasa.gov

Glen Mucklow

Office of Space Sciences (Code SM)
(202) 358-2235 or
gmucklow@nasa.gov

Roger Crouch

Office of Microgravity Science Applications (Code U)
(202) 358-0689 or
rcrouch@nasa.gov

Granville Paules

Office of Mission to Planet Earth (Code Y)
(202) 358-0706 or
gpaules@mtpe.hq.nasa.gov



TECH BRIEFS

NATIONAL AERONAUTICS AND SPACE ADMINISTRATION



5 Technology Focus: Sensors

- 5 Relative-Motion Sensors and Actuators for Two Optical Tables
- 6 Improved Position Sensor for Feedback Control of Levitation
- 7 Compact Tactile Sensors for Robot Fingers
- 7 Improved Ion-Channel Biosensors



9 Electronics/Computers

- 9 Suspended-Patch Antenna With Inverted, EM-Coupled Feed
- 10 System Would Predictively Preempt Traffic Lights for Emergency Vehicles
- 11 Optical Position Encoders for High or Low Temperatures
- 12 Inter-Valence-Subband/Conduction-Band-Transport IR Detectors
- 13 Additional Drive Circuitry for Piezoelectric Screw Motors



15 Software

- 15 Software for Use With Optoelectronic Measuring Tool
- 15 Coordinating Shared Activities
- 15 Software Reduces Radio-Interference Effects in Radar Data



17 Materials

- 17 Using Iron To Treat Chlorohydrocarbon-Contaminated Soil



19 Mechanics

- 19 Thermally Insulating, Kinematic Tensioned-Fiber Suspension

- 20 Back Actuators for Segmented Mirrors and Other Applications

- 20 Mechanism for Self-Reacted Friction Stir Welding



23 Machinery/Automation

- 23 Lightweight Exoskeletons With Controllable Actuators
- 24 Miniature Robotic Submarine for Exploring Harsh Environments



25 Physical Sciences

- 25 Electron-Spin Filters Based on the Rashba Effect
- 26 Diffusion-Cooled Tantalum Hot-Electron Bolometer Mixers
- 27 Tunable Optical True-Time Delay Devices Would Exploit EIT



29 Information Sciences

- 29 Fast Query-Optimized Kernel-Machine Classification
- 29 Indentured Parts List Maintenance and Part Assembly Capture Tool — IMPACT
- 30 An Architecture for Controlling Multiple Robots



33 Books & Reports

- 33 Progress in Fabrication of Rocket Combustion Chambers by VPS
- 33 CHEM-Based Self-Deploying Spacecraft Radar Antennas
- 33 Scalable Multiprocessor for High-Speed Computing in Space
- 33 Simple Systems for Detecting Spacecraft Meteoroid Punctures

This document was prepared under the sponsorship of the National Aeronautics and Space Administration. Neither the United States Government nor any person acting on behalf of the United States Government assumes any liability resulting from the use of the information contained in this document, or warrants that such use will be free from privately owned rights.



Relative-Motion Sensors and Actuators for Two Optical Tables

Relative motions can be suppressed or imposed on demand.

NASA's Jet Propulsion Laboratory, Pasadena, California

Optoelectronic sensors and magnetic actuators have been developed as parts of a system for controlling the relative position and attitude of two massive optical tables that float on separate standard air suspensions that attenuate ground vibrations. In the specific application for which these sensors and actuators were developed, one of the optical tables holds an optical system that mimics distant stars, while the other optical table holds a test article that simulates a spaceborne stellar interferometer that would be used to observe the stars.

The control system is designed to suppress relative motion of the tables or, on demand, to impose controlled relative motion between the tables. The control system includes a sensor system that detects relative motion of the tables in six independent degrees

of freedom and a drive system that can apply force to the star-simulator table in the six degrees of freedom.

The sensor system (see Figure 1) includes (1) a set of laser heterodyne gauges and (2) a set of four diode lasers on the star-simulator table, each aimed at one of four quadrant photodiodes at nominal corresponding positions on the test-article table. The heterodyne gauges are used to measure relative displacements along the x axis.

The most innovative part of the sensor system is the quadrant-photodetector subsystem, which differs from commercial quadrant-photodetector relative-position-measuring systems. The active area of each quadrant photodiode is 1 cm in diameter. The 635-nm-wavelength output of each laser diode is coupled via an optical fiber to a collimator, which focuses the laser beam to a spot centered

at the nominal center of the corresponding quadrant photodiode. The laser spots on two of the quadrant photodiodes are 5 mm in diameter; these quadrant photodiodes provide low-resolution, high-dynamic range measurements of relative displacements and tilts in the y-z plane. These measurements are used to bring the tables into coarse alignment. The laser spots on the remaining two quadrant photodiodes are 0.55 mm in diameter; these quadrant photodiodes provide high-resolution, low-dynamic range measurements of relative displacements and tilts in the y-z plane, thereby enabling finer alignment. This quadrant-photodiode subsystem offers two advantages over commercial quadrant-photodetector relative-position-measuring systems: it is much quieter (its position noise output is about a hundredth of that of a typical com-

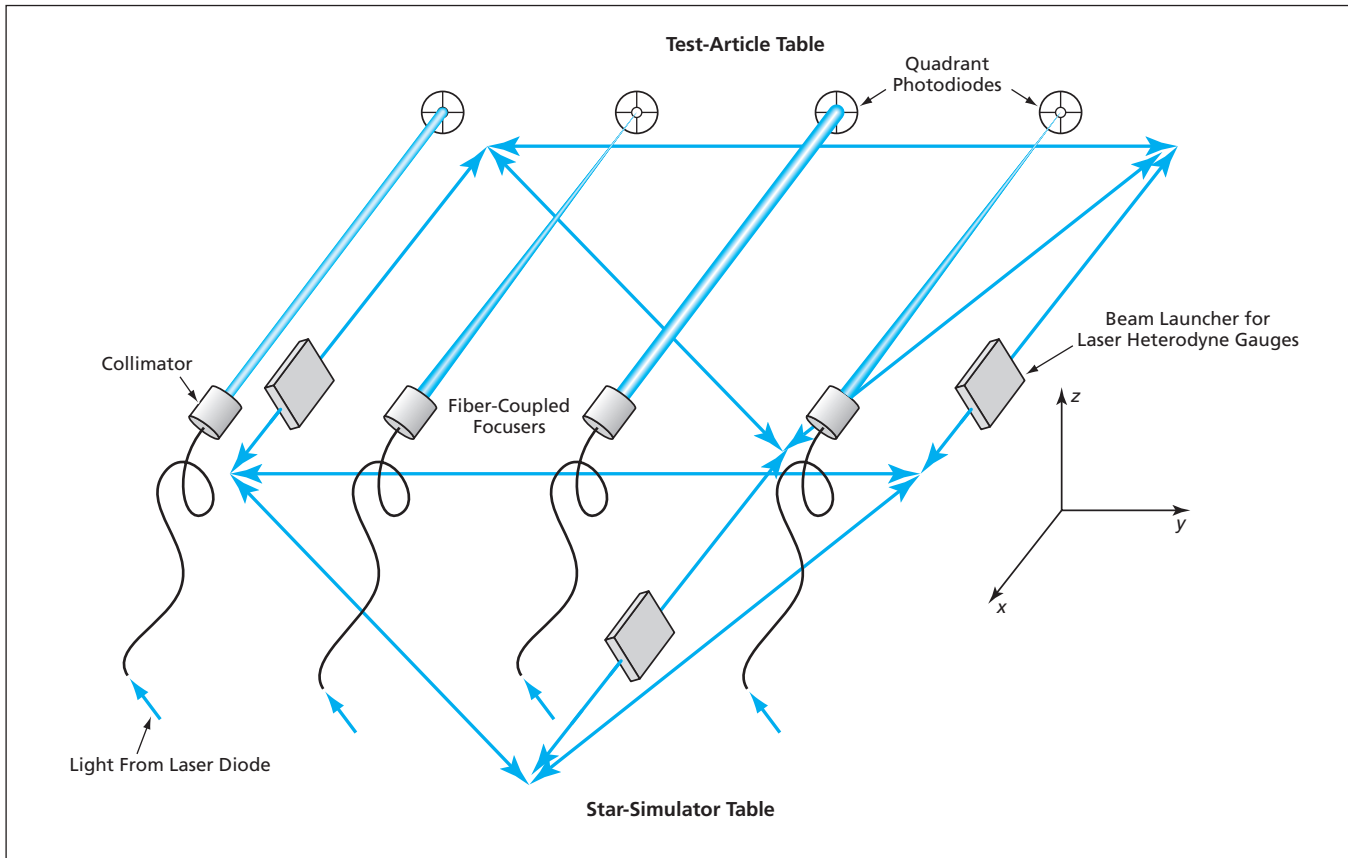


Figure 1. Two Optoelectronic Sensor Subsystems use collimated laser beams to measure relative motions of the star-simulator and test-article tables.

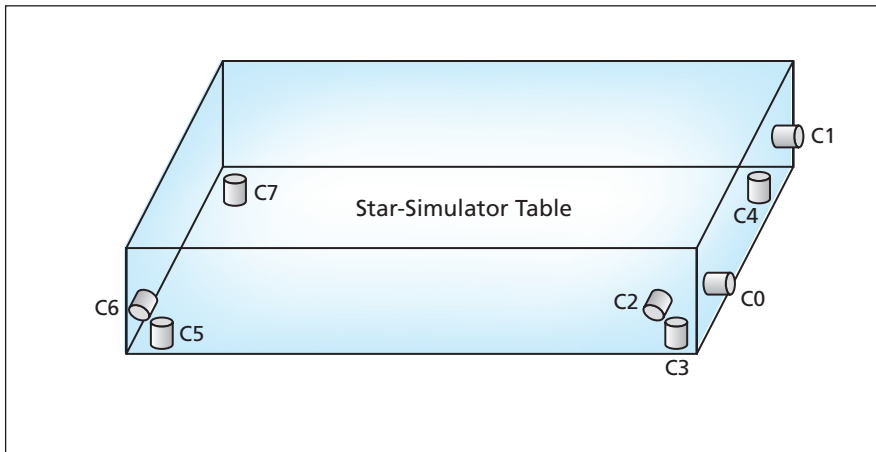


Figure 2. **Eight Linear Magnetic Actuators**, partly similar to traditional voice-coil actuators, apply forces to the star-simulator table to control its position and attitude in all six degrees of freedom. The actuators are represented by the cylinders labeled C0 through C7.

mercial system) and it can be constructed at relatively low cost.

The drive system includes eight magnetic linear actuators — two more than the minimum of six needed for the six

degrees of freedom. Each actuator partly resembles a traditional voice-coil actuator in that it includes a permanent magnet, upon which an axial force is exerted by a nominally concen-

tric electromagnet coil. The force exerted by each actuator depends on the current applied to its coil and typically lies in the range of ± 10 N (for some degrees of freedom, the typical range is ± 40 N). Unlike a traditional voice-coil actuator, which cannot withstand a lateral displacement of more than 0.1 mm without breakage, each of these magnetic actuators can withstand a displacement of ± 5 mm in any direction without breakage. The electromagnet coils are wound on aluminum forms that contain water cooling channels to remove excess heat from the coils when necessary. The motions of the permanent magnets in the aluminum forms also provide eddy-current damping of rapid motions (e.g., vibrations) of the table.

This work was done by Yekta Gursel and Elizabeth McKenney of Caltech for NASA's Jet Propulsion Laboratory. Further information is contained in a TSP (see page 1). NPO-30805

Improved Position Sensor for Feedback Control of Levitation

In this application, an incandescent light bulb is preferable to a laser.

Marshall Space Flight Center, Alabama

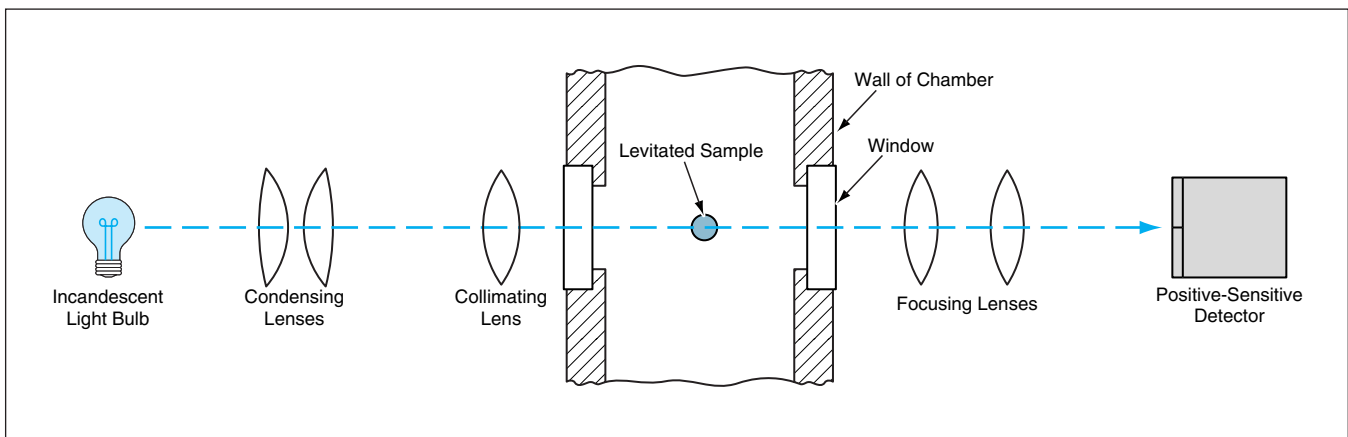
An improved optoelectronic apparatus has been developed to provide the position feedback needed for controlling the levitation subsystem of a containerless-processing system. As explained below, the advantage of this apparatus over prior optoelectronic apparatuses that have served this purpose stems from the use of an incandescent lamp, instead of a laser, to illuminate the levitated object.

In containerless processing, a small object to be processed is levitated (e.g.,

by use of a microwave, low-frequency electromagnetic, electrostatic, or acoustic field) so that it is not in contact with the wall of the processing chamber or with any other solid object during processing. In the case of electrostatic or low-frequency electromagnetic levitation, real-time measurement of the displacement of the levitated object along the vertical axis (and, in some cases, along one or two horizontal axes)

is needed for feedback control of the levitating field.

In a typical prior position-measuring optoelectronic apparatus for levitation control, a laser beam is aimed through the nominal levitation position to a position-sensitive photodetector, so that the levitated object casts a shadow on the detector face. The output of the position-sensitive detector circuitry is a voltage proportional to the displacement of the shadow from a nominal



An **Incandescent Light Bulb** and some lenses are used to illuminate a levitated object in a processing chamber so that the object casts a shadow on a position-sensitive detector.

central position and, hence, to the displacement of the levitated object from the nominal levitation position. The main shortcomings of such an apparatus are associated with the laser: Lasers tend to be expensive, and laser beams are often characterized by poor spatial distribution (speckle) and by poor short-term spatial and temporal stability.

The basic principle of operation of the improved optoelectronic position-measuring apparatus is the same as that of the prior apparatus described above,

except that the laser is replaced with an incandescent light bulb and associated optics (see figure). Unlike the light from a laser, the light from an incandescent lamp is not subject to mode shifts and, hence, is spatially and temporally stable in the short term. The spatial distribution of light is better for the intended application because there is no speckle and the illumination is approximately constant across the levitation region. Unlike the light from a laser, the light from an incandescent lamp varies smoothly with applied

power and is thus more easily controllable. Finally, a light bulb is easily replaceable and costs much less than does a laser.

This work was done by Robert Hyers, Larry Savage, and Jan Rogers of Marshall Space Flight Center.

This invention is owned by NASA, and a patent application has been filed. For further information, contact Benita Hayes, MSFC Commercialization Assistance Lead, at benita.c.hayes@nasa.gov. Refer to MFS-31535.

Compact Tactile Sensors for Robot Fingers

Simple, rugged, compact sensors measure spatial distributions of contact forces.

Lyndon B. Johnson Space Center, Houston, Texas

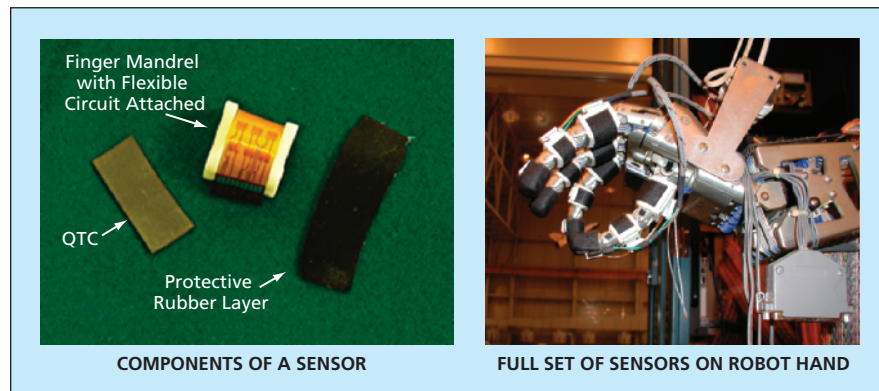
Compact transducer arrays that measure spatial distributions of force or pressure have been demonstrated as prototypes of tactile sensors to be mounted on fingers and palms of dexterous robot hands. The pressure- or force-distribution feedback provided by these sensors is essential for the further development and implementation of robot-control capabilities for humanlike grasping and manipulation.

Each sensor (see figure) includes a hard mandrel designed to fit over a finger segment or a palm. A flexible circuit that includes an array of electrodes is attached to the mandrel and is overlaid with a force-sensitive rubber denoted quantum-tunneling composite (QTC). A protective layer of non-sensory rubber is placed over the QTC.

Each electrode defines a tactile sensor point denoted a tactel in analogy to a

pixel (picture element) in an image-detecting array of photodetectors. In addition to the electrodes, the sensor includes a ground conductor common to all the elements of the array. The local electrical resistivity of the QTC changes in response to local pressure. By use of simple electronic circuits (e.g., resistive voltage dividers), the local changes of resistance in the tactels are converted to voltages. The voltages can be read by use of external analog-to-digital converter circuitry, then processed into forces or pressures on the tactels. Hence, the processed sensor output indicates the spatial distribution of force or pressure at the spatial resolution of the tactels.

This work was done by Toby B. Martin of Johnson Space Center; David Lussey of Peratech, Ltd.; Frank Gaudiano, Aaron Hulse, Myron A. Diftler, and Dagoberto Rodriguez of Lockheed Martin Corp.; Paul Biel-ski of Titan Systems Corp.; and Melisa Butzer of Oceaneering Space Systems. For further information, contact the Johnson Commercial Technology Office at (281) 483-3809. MSC-23608/93



A Sensor for a Finger includes a hard mandrel that fits over the finger and that supports a flexible circuit overlaid by a QTC overlaid by protective rubber.

Improved Ion-Channel Biosensors

Improvements include greater stability and greater signal-to-noise ratios.

NASA's Jet Propulsion Laboratory, Pasadena, California

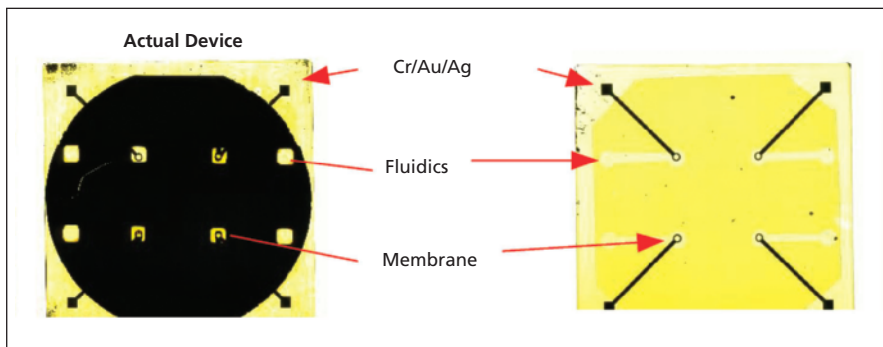
An effort is underway to develop improved biosensors of a type based on ion channels in biomimetic membranes. These sensors are microfabricated from silicon and other materials compatible

with silicon. As described below, these sensors offer a number of advantages over prior sensors of this type.

To place these advantages in context, it is first necessary to present some back-

ground information on prior sensors of this type:

- Ion channels of the type in question are very sensitive to a wide variety of ligands, to which they respond by gen-



An Array of Four Wells containing sensor structures was fabricated in a silicon wafer of 4-in. (≈ 10 -cm) diameter to demonstrate the ability to make an array of multiple sensors on a single chip. Each sensor is electrically addressed, separately from the other sensors, via its electrodes.

erating specific electrical signals. Consequently, such ion channels would be ideal bases for biosensors if they could be constructed in arrays and made stable and electrically addressable.

- Unfortunately, such ion channels function only within biological or biomimetic membranes, the life spans of which, heretofore, have usually been no more than several hours. In addition, their small signals (currents of 1 to 10 pA) make it necessary to mount them on platforms along with, and coupled to, low-noise, highly-amplifying electronic circuits. These characteristics have posed difficulties that have limited the commercial development of ion-channel biosensors.
- Heretofore, the standard design of one commercial product line of ion-channel recording devices has provided for lipid-bilayer recording chambers. Such chambers are suitable for short-term (1 to 2 hours) recording only and are not constructed in arrays. Another commercial product line of ion-channel biosensors offers

the stability needed for longer-term recording, but operation is limited to DC capacitive measurements.

The figure presents top and bottom views of a prototype array of four of the developmental sensors fabricated in a silicon wafer on a glass plate. Each sensor in the array can be individually electrically addressed, without interference with its neighbors. Each sensor includes a well covered by a thin layer of silicon nitride, in which is made a pinhole for the formation of lipid bilayer membrane. In one stage of fabrication, the lower half of the well is filled with agarose, which is allowed to harden. Then the upper half of the well is filled with a liquid electrolyte (which thereafter remains liquid) and a lipid bilayer is painted over the pinhole. The liquid contains a protein that forms an ion-channel on top of the hardened agarose. The combination of enclosure in the well and support by the hardened agarose provides the stability needed to keep the membrane functional for times as long as days or even weeks.

An electrode above the well, another electrode below the well, and all the materials between the electrodes together constitute a capacitor. What is measured is the capacitive transient current in response to an applied voltage pulse. One notable feature of this sensor, in comparison with prior such sensors, is a relatively thick dielectric layer between the top of the well and the top electrode. This layer greatly reduces the capacitance of an aperture across which the ion channels are formed, thereby increasing the signal-to-noise ratio. The use of a relatively large aperture with agarose support makes it possible to form many ion channels instead of only one, thereby further increasing the signal-to-noise ratio and effectively increasing the size of the available ionic reservoir. The relatively large reservoir makes it possible to measure AC rather than DC.

This work was done by Jay Nadeau, Victor White, Dennis Dougherty, and Joshua Maurer of Caltech for NASA's Jet Propulsion Laboratory. Further information is contained in a TSP (see page 1).

In accordance with Public Law 96-517, the contractor has elected to retain title to this invention. Inquiries concerning rights for its commercial use should be addressed to:

*Innovative Technology Assets Management
JPL*

*Mail Stop 202-233
4800 Oak Grove Drive
Pasadena, CA 91109-8099
(818) 354-2240*

E-mail: iaoffice@jpl.nasa.gov

Refer to NPO-30710, volume and number of this NASA Tech Briefs issue, and the page number.



Suspended-Patch Antenna With Inverted, EM-Coupled Feed

This design offers advantages with respect to efficiency, fabrication, cost, and weight.

John H. Glenn Research Center, Cleveland, Ohio

An improved suspended-patch antenna has been designed to operate at a frequency of about 23 GHz with linear polarization and to be one of four identical antennas in a rectangular array. The antenna (see Figure 1) includes a parasitic patch on top of a suspended dielectric superstrate, an active patch on top of a suspended dielectric substrate, a microstrip on the bottom of the dielectric substrate, and a ground plane. The microstrip, the ground plane, the airgap between them, and the dielectric substrate together constitute a transmission line that has an impedance of 50 Ω and is electromagnetically (EM) coupled to the active patch. The parasitic patch is, in turn, excited by the active patch. The microstrip feed is characterized as inverted because the microstrip is on the bottom of the substrate, whereas microstrips are usually placed on the tops of dielectric substrates.

The advantages of this design are the following:

- The attenuation in the inverted microstrip feed is less than that of a conventional microstrip feed; hence, the conductor loss associated with the corporate feed of the antenna is correspondingly lower and the gain and efficiency of the antenna are correspondingly higher.
- Relative to a conventional microstrip feed, the inverted microstrip feed can be fabricated more easily because the strip width for a given characteristic impedance is greater.
- Whereas a conventional EM-coupled patch antenna includes a dielectric substrate for the microstrip feed and another suspended dielectric layer for the active patch, one dielectric substrate supports both the microstrip and the active patch in this antenna. The elimination of the additional suspended dielectric layer reduces the weight and cost of the antenna.

- The electromagnetic coupling affords greater bandwidth than does conductive coupling.

Figure 2 presents measurements performed on the four-antenna array. The return-loss plot shows that the array is very well matched to the 50- Ω feed lines. The relative bandwidth for return loss ≤ -10 dB is about 5.4 percent. The array was found to radiate with substantially linear polarization. The measured gain of the array, as compared with that of a standard gain horn antenna, is estimated to be about 10 dB.

This work was done by Rainee N. Simons of Dynacs Engineering Co. for Glenn Research Center. Further information is contained in a TSP (see page 1).

Inquiries concerning rights for the commercial use of this invention should be addressed to: NASA Glenn Research Center, Commercial Technology Office, Attn: Steve Fedor, Mail Stop 4-8, 21000 Brookpark Road, Cleveland, Ohio 44135.

Refer to LEW-17354.

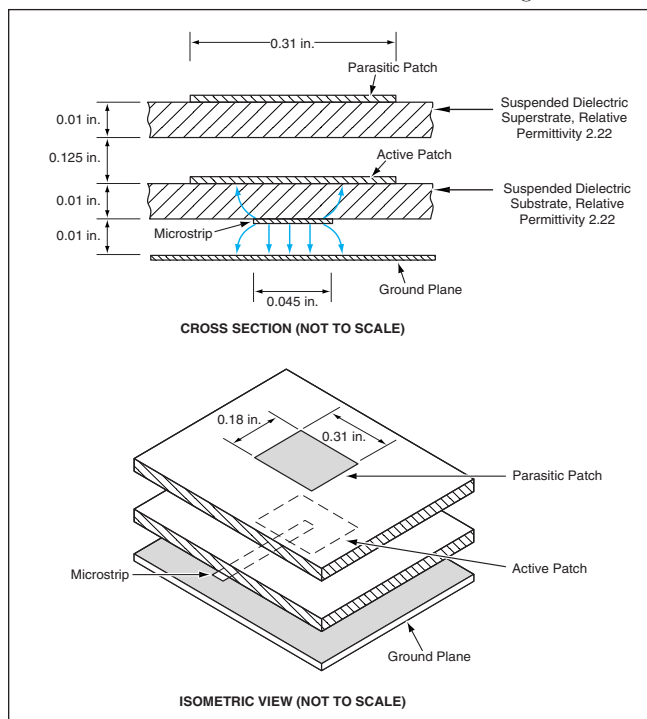


Figure 1. The Dielectric and Conductive Layers in this antenna are arranged to reduce losses, relative to comparable prior patch antennas that include EM-coupled elements. The dimensions shown are for a design frequency of ≈ 23 GHz.

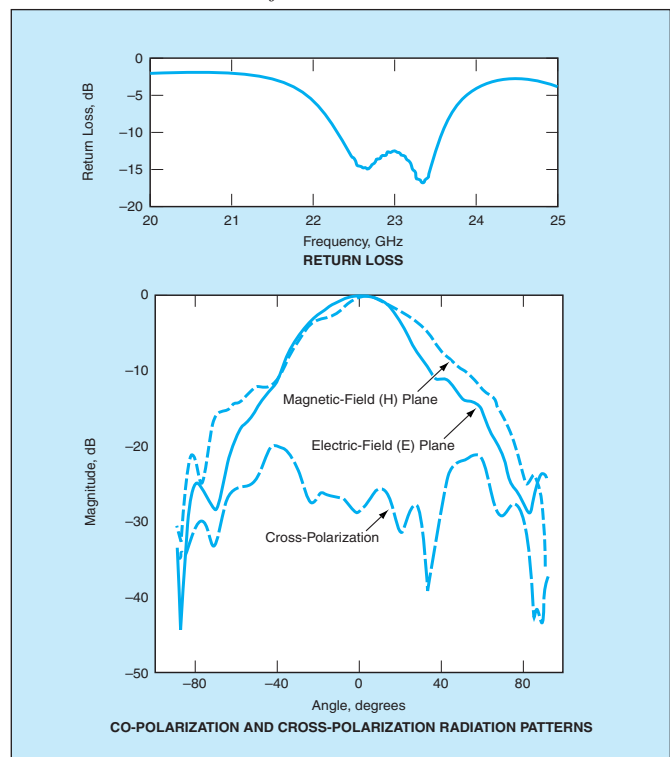


Figure 2. Return Loss and Radiation Patterns were measured for a rectangular array of four antennas like that of Figure 1.

System Would Predictively Preempt Traffic Lights for Emergency Vehicles

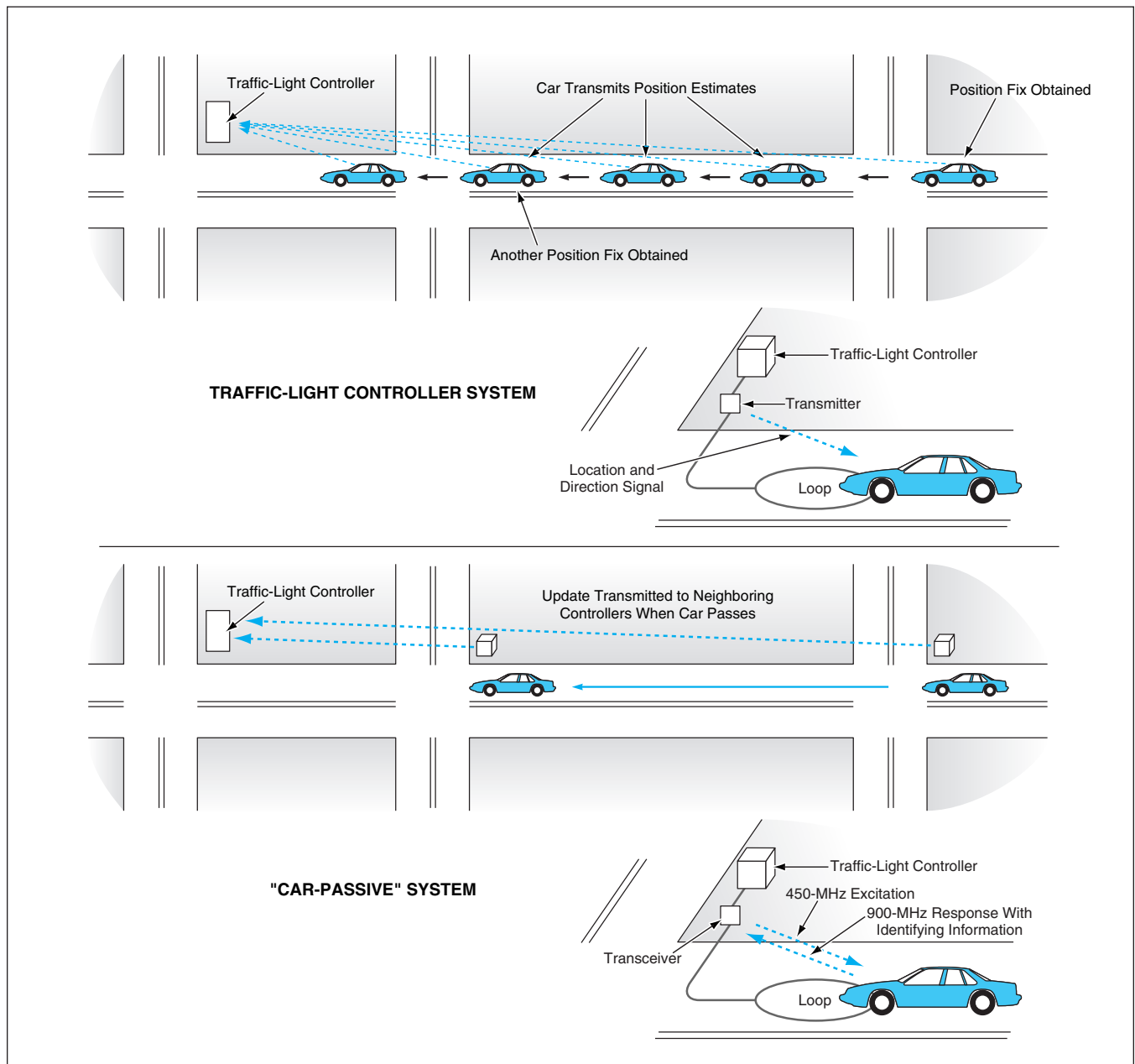
These systems could utilize traffic-light infrastructure already in place.

NASA's Jet Propulsion Laboratory, Pasadena, California

Two electronic communication-and-control systems have been proposed as means of modifying the switching of traffic lights to give priority to emergency vehicles. Both systems would utilize the inductive loops already installed in the streets of many municipalities to detect vehicles for timing the switching of traffic lights. The proposed systems could

be used alone or to augment other automated emergency traffic-light preemption systems that are already present in some municipalities, including systems that recognize flashing lights or siren sounds or that utilize information on the positions of emergency vehicles derived from the Global Positioning System (GPS). Systems that detect flashing

lights and siren sounds are limited in range, cannot "see" or "hear" well around corners, and are highly vulnerable to noise. GPS-based systems are effective in rural areas and small cities, but are often ineffective in large cities because of frequent occultation of GPS satellite signals by large structures. In contrast, the proposed traffic-loop for-



Traffic Lights Would Be Preempted for emergency vehicles by a "car-active" or a "car-passive" system. Both systems would utilize inductive traffic loops already installed in the streets of many municipalities.

ward prediction system would be relatively invulnerable to noise, would not be subject to significant range limitations, and would function well in large cities — even in such places as underneath bridges and in tunnels, where GPS-based systems do not work.

One proposed system has been characterized as “car-active” because each participating emergency vehicle would be equipped with a computer and a radio transceiver that would communicate with stationary transceivers at the traffic loops (see figure). Whenever a vehicle was detected passing over a traffic loop, the loop transceiver, possibly using the loop as an antenna, would transmit a signal identifying the location of the loop and the direction of travel. (Traffic-loop equipment that performs this function is already commercially available.) If the vehicle passing over the loop were a participating vehicle, its transceiver would receive the position signal. The computer in the vehicle would use the signal and the time of its receipt as a time-and-position fix in a continuous “dead reckoning” estimation of the cur-

rent position of the vehicle as function of speed and compass heading. At time intervals of 1 second, the transceiver would broadcast the updated estimate of position to loop receivers at neighboring intersections. The stationary portion of the system would determine, on the basis of the updates, whether the vehicle was likely to pass through a given intersection within a suitable amount of time (typically of the order of 1 minute), in which case the system would preempt the switching of traffic lights at the intersection.

The other proposed system has been characterized as “car-passive” because a passive radio transponder would be installed on the underside of a participating vehicle. When passing over a traffic loop, the transponder would be energized by a signal, at a frequency of 450 MHz, radiated via the loop. When so energized, the transponder would transmit a vehicle identification number signal at a carrier frequency of 900 MHz. Unlike in the car-active system, there would be no continuous estimation of vehicle position. Instead, traffic lights would be

preempted on the basis of simple proximity detection. For this purpose, upon detection of a participating vehicle at a loop at a given intersection, the detection would be signaled to neighboring intersections. Traffic lights at the next intersection or next few intersections through which the vehicle could be expected to pass could then be preempted until the vehicle passed through or until a specified time elapsed.

This work was done by Aaron Bachelder and Conrad Foster of Caltech for NASA's Jet Propulsion Laboratory. Further information is contained in a TSP (see page 1).

In accordance with Public Law 96-517, the contractor has elected to retain title to this invention. Inquiries concerning rights for its commercial use should be addressed to:

*Intellectual Assets Office
JPL, Mail Stop 202-233
4800 Oak Grove Drive
Pasadena, CA 91109
(818) 354-2240
E-mail: ipgroup@jpl.nasa.gov
Refer to NPO-30573, volume and number of this NASA Tech Briefs issue, and the page number.*

Optical Position Encoders for High or Low Temperatures

CCD cameras monitor backlit scales via coherent fiber-optic bundles.

Goddard Space Flight Center, Greenbelt, Maryland

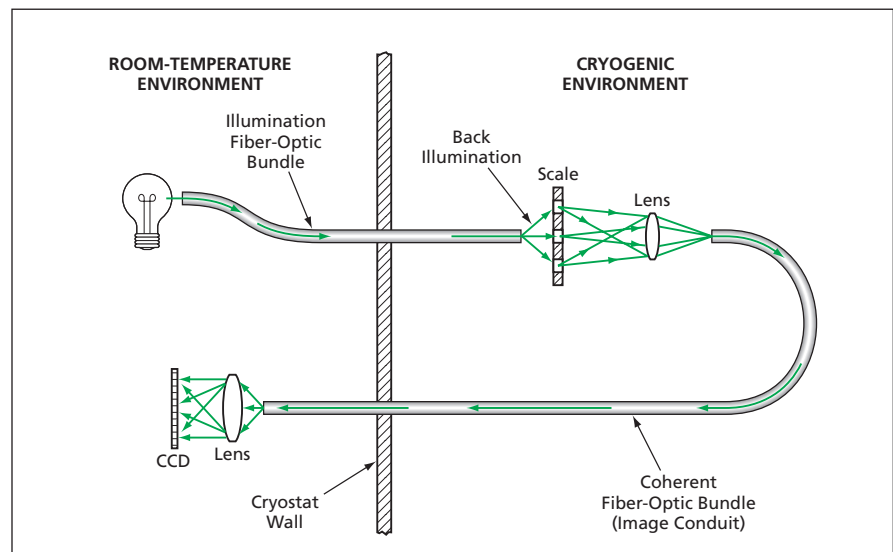
Optoelectronic pattern-recognition systems (optical encoders) for measuring positions of objects of interest at temperatures well below or well above room temperature are undergoing development. At present, the development effort is concentrated on absolute linear, rotary, and Cartesian encoders and Cartesian autocollimators for scientific instruments that operate in cryostats.

Like some prior pattern-recognition optical encoders, a system of the present type includes a backlit scale attached to the object of interest, a charge-coupled-device (CCD) camera, a lens to project a possibly magnified image of the scale onto the CCD, circuitry to digitize the image detected by CCD, and a computer to process the image data to determine positions of the optically projected scale marks in the reference frame embodied in the array of pixels of the CCD. Unlike in prior systems, neither the light source for illuminating the scale nor the CCD is located in the cold or hot environment that contains the object of interest and the attached scale. This arrangement

makes it possible for the CCD to read the scale even though the CCD could not function properly if it were located in that environment. In the case of a cryogenic environment, this arrangement is particularly advantageous because it min-

imizes spurious heating by the light source and eliminates spurious heating that would otherwise be caused by dissipation of power in the CCD circuitry.

A cryogenic implementation of a linear or rotary encoder of this type is con-



Fiber-Optic Bundles are used to feed light to and from a position-encoding scale in a cryostat.

ceptually straightforward (see figure). By use of a conventional illumination-type fiber-optic bundle, visible light from a source outside a cryostat is fed into the cryostat to back-illuminate the scale. In a typical case, an image of the scale can be acquired and fed to the CCD optics by use of a lens-tipped coherent fiber-optic bundle similar to a fiber-optic borescope or endoscope. A low-thermal-conductiv-

ity hermetic feedthrough is installed at the point where the fiber-optic bundle passes through the cryostat wall. Alternately, an image of the scale can be projected out through a small window in the cryostat wall. Either way, the encoding function involves very little energy dissipation inside the cryostat.

This work was done by Douglas B. Leviton of Goddard Space Flight Center. Further

information is contained in a TSP (see page 1).

This invention is owned by NASA, and a patent application has been filed. Inquiries concerning nonexclusive or exclusive license for its commercial development should be addressed to the Patent Counsel, Goddard Space Flight Center, (301) 286-7351. Refer to GSC-14766-1.

Inter-Valence-Subband/Conduction-Band-Transport IR Detectors

These devices would be capable of operation at normal incidence.

NASA's Jet Propulsion Laboratory, Pasadena, California

Infrared (IR) detectors characterized by a combination of (1) high-quantum-efficiency photoexcitation of inter-valence-subband transitions of charge carriers and (2) high-mobility conduction-band transport of the thus-excited charge carriers have been proposed in an effort to develop focal-plane arrays of such devices for infrared imaging. Like many prior quantum-well infrared photodetectors (QWIPs), the proposed devices would be made from semiconductor heterostructures. In order to obtain the combination of characteristics mentioned above, the proposed devices would be designed and fabricated in novel InAs/GaSb superlattice configurations that would exploit a phenomenon known in the semiconductor art as type-II broken-gap band offset.

Previously tested GaInSb/InAs type-II strained-layer-superlattice devices have shown the potential to offer optical properties comparable to, degrees of uniformity greater than, and tunneling currents and Auger recombination less than, those of HgCdTe IR photodetectors. Moreover, the GaInSb/InAs type-II strained-layer devices have been shown to be capable of

operation at normal incidence. The operation of the GaInSb/InAs type-II strained-layer devices involves transitions from valence subbands in GaInSb to conduction subbands in InAs. The spatial separation of wave functions involved in the transition results in reduced oscillator strengths. Therefore, to obtain adequate quantum efficiency, it is necessary to grow thick, high-quality superlattices — a task that is challenging because GaInSb and InAs are lattice-mismatched. The development of the proposed devices would implement an alternative approach to exploitation of some of the same basic principles as those of the GaInSb/InAs type-II strained-layer devices.

It is useful to compare the proposed GaSb/InAs QWIPs with prior GaAs/AlGaAs QWIPs, which utilize n doping. Because quantum-mechanical selection rules in n-doped QWIPs forbid inter-conduction-subband transitions induced by normally incident light, optical coupling gratings are needed to achieve acceptable quantum efficiencies in such QWIPs. On the other hand, inter-valence-subband transitions in p-doped QWIPs can absorb normally incident photons with

high quantum efficiency, so that optical coupling gratings are not needed.

An InAs/GaSb multi-quantum well structure according to the proposal would comprise p-doped GaSb quantum wells embedded in InAs barriers (see figure). The inter-valence-subband transitions in the GaSb wells would absorb normally incident photons with high quantum efficiency. Although the InAs layers would be barriers to ground-state electrons, a device of this type would take advantage of the high electron mobility in the InAs conduction band for transporting excited electrons between the GaSb quantum wells. This would be made possible by the type-II broken-gap band offset between InAs and GaSb: The edge of the valence band of GaSb is approximately 0.15 eV higher than the conduction-band edge of InAs. Therefore, electrons in the p-doped GaSb quantum wells that were photoexcited to the uppermost subband (denoted the heavy-hole 1 or hh1 subband) could easily escape into the conduction band in InAs layers.

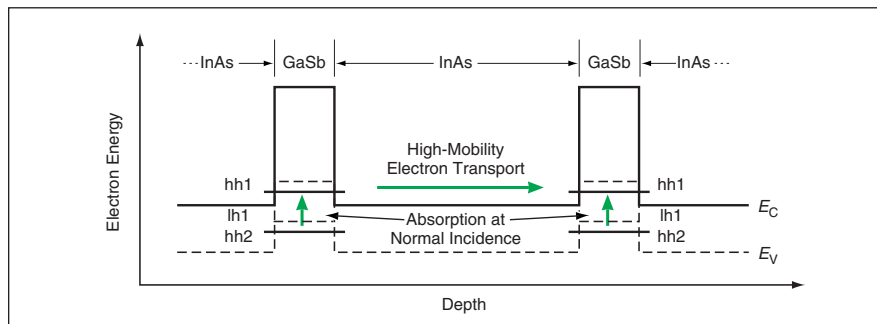
This work was done by David Ting, Sarath Gunapala, and Sumith Bandara of Caltech for NASA's Jet Propulsion Laboratory. Further information is contained in a TSP (see page 1).

In accordance with Public Law 96-517, the contractor has elected to retain title to this invention. Inquiries concerning rights for its commercial use should be addressed to:

*Innovative Technology Assets Management
JPL
Mail Stop 202-233
4800 Oak Grove Drive
Pasadena, CA 91109-8099
(818) 354-2240*

E-mail: iaoffice@jpl.nasa.gov

Refer to NPO-30426, volume and number of this NASA Tech Briefs issue, and the page number.



This Energy-Band Diagram of a GaSb/InAs QWIP depicts the energy levels involved in the exploitation of (1) inter-valence-subband transitions in GaSb for detection and (2) transport in the InAs conduction band. The relevant energy bands and the energies at their edges are denoted as follows: EC for conduction band; EV for valence band; hh1 and hh2 for heavy-hole bands 1 and 2, respectively; and lh1 for light-hole band 1.

Additional Drive Circuitry for Piezoelectric Screw Motors

A single driver can be used to control as many as 16 motors.

NASA's Jet Propulsion Laboratory, Pasadena, California

Modules of additional drive circuitry have been developed to enhance the functionality of a family of commercially available positioning motors (Picomotor™ or equivalent) that provide linear motion controllable, in principle, to within increments ≤ 30 nm. A motor of this type includes a piezoelectric actuator that turns a screw. Unlike traditional piezoelectrically actuated mechanisms, a motor of this type does not rely on the piezoelectric transducer to hold position: the screw does not turn except when the drive signal is applied to the actuator.

In the original application for which these modules were developed, a clockwise-vs.-counterclockwise asymmetry in the pulses generated by a driver module that operates at a rate of ≤ 1 kHz made it impossible to reliably command the advertised ≤ 30 -nm steps in either direction. In addition, the original application in-

cluded low-duty-cycle operation, which offered the opportunity to reduce cost by using a single driver module with multiplexing circuitry to drive several motors. There was an additional desire to modify the motors by integrating limit switches into them to provide calibration and position-reference signals.

Because of the highly specific nature of its origin, a module of the present type is denoted a Picomotor break-out box. It is designed to be installed and operated in conjunction with (1) an improved, high-voltage driver module, developed specifically for use with a motor of the type in question, that operates at a rate ≤ 2 kHz; (2) a commercial digital input/output module; and (3) a commercial counter/timer module. Among other things, a Picomotor break-out box affords a capability for multiplexing of output for low-duty-cycle control of as

many as 16 motors. The circuitry in the break-out box includes a commercial gate array that can be triggered by a limit switch to immediately stop the pulse train fed to the driver module, thereby eliminating what would otherwise be the latency involved in stopping motion via software. Also included in the break-out box are power supplies for the driver module and accessory signal boards. The break-out box and the driver box are connected by a single cable that can be up to 130 feet (39.6 m) long, so the thermal pollution of the power supplies can be physically isolated from the actuators.

This work was done by Robert Smythe, Dean Palmer, Yekta Gursel, Leonard Reder, and Raymond Savedra of Caltech for NASA's Jet Propulsion Laboratory. Further information is contained in a TSP (see page 1). NPO-30359

Software for Use With Optoelectronic Measuring Tool

A computer program has been written to facilitate and accelerate the process of measurement by use of the apparatus described in "Optoelectronic Tool Adds Scale Marks to Photographic Images" (KSC-12201), *NASA Tech Briefs*, Vol. 27, No. 1 (January 2003), page 6a. To recapitulate: The tool contains four laser diodes that generate parallel beams of light spaced apart at a known distance. The beams of light are used to project bright spots that serve as scale marks that become incorporated into photographic images (including film and electronic images). The sizes of objects depicted in the images can readily be measured by reference to the scale marks.

The computer program is applicable to a scene that contains the laser spots and that has been imaged in a square pixel format that can be imported into a graphical user interface (GUI) generated by the program. It is assumed that the laser spots and the distance(s) to be measured all lie in the same plane and that the plane is perpendicular to the line of sight of the camera used to record the image. The user marks the locations of the laser spots in the image, and the program calculates the distance (L_s) between them in pixels as simply the square root of the sum of squares of the horizontal and vertical pixel distances between them. Similarly, the user marks any two points, the distance between which is to be measured, and the program calculates the distance (P_s) between them in pixels, in the same manner in which it calculates the pixel distance between the laser spots. Then the program calculates the real distance (L_o) between the two points by $L_o = L_s P_o / P_s$, where L_s is the known real distance between the laser spots.

The original version of the program, written in Fortran, offered limited performance: it could accept only bit-map (BMP) image data files and was somewhat awkward to use. The current version, written in C++, performs better, in part because it utilizes capabilities afforded by the Windows operating system. In addition to BMP files, the program can now read and save image files in the Joint Photographic Experts Group (JPEG or JPG) and Graphic Image File (GIF) formats. Some of the

other features of the current version of the software are the following:

- The GUI has been made less complex and is easier to use than it was in the original version.
- The total number of laser-spot marks that the user can place in the image is not limited to four. Moreover, the marks need not be limited in application to the laser spots: they can be applied to any linear set of evenly spaced reference marks (for example, a row of evenly spaced screw heads) as long as the distance between the marks is known.
- A given pair of measurement points and a rectangular measurement zone bounded by two points at diagonally opposite corners is established by stretching the straight diagonal line between them in a conventional point-and-click "rubber band" mouse operation. The GUI displays the horizontal, vertical, and diagonal dimensions of the measurement zone as the mouse is dragged to stretch the diagonal.
- By means of a "Set Actual Distance" command, the user can prescribe or update the distance along the diagonal of a measurement zone. The updated actual diagonal horizontal, vertical, and diagonal distance values are immediately displayed in the image. In addition, a status bar provides an option to display the actual distance between laser spots.
- Context-sensitive help displays comprising text, images, and hypertext links to related pages are available for each command and GUI button. There is also a help page describing the procedure for using the program.

This program was written by Kim C. Ballard of Kennedy Space Center. Further information is contained in a TSP (see page 1).

This invention is owned by NASA, and a patent application has been filed. Inquiries concerning nonexclusive or exclusive license for its commercial development should be addressed to the Technology Programs and Commercialization Office, Kennedy Space Center, (321) 867-8130. Refer to KSC-12505.

Coordinating Shared Activities

Shared Activity Coordination (ShAC) is a computer program for planning and scheduling the activities of an autonomous team of interacting spacecraft

and exploratory robots. ShAC could also be adapted to such terrestrial uses as helping multiple factory managers work toward competing goals while sharing such common resources as floor space, raw materials, and transports. ShAC iteratively invokes the Continuous Activity Scheduling Planning Execution and Replanning (CASPER) program to replan and propagate changes to other planning programs in an effort to resolve conflicts. A domain-expert specifies which activities and parameters thereof are shared and reports the expected conditions and effects of these activities on the environment. By specifying these conditions and effects differently for each planning program, the domain-expert subprogram defines roles that each spacecraft plays in a coordinated activity. The domain-expert subprogram also specifies which planning program has scheduling control over each shared activity. ShAC enables sharing of information, consensus over the scheduling of collaborative activities, and distributed conflict resolution. As the other planning programs incorporate new goals and alter their schedules in the changing environment, ShAC continually coordinates to respond to unexpected events.

This program was written by Bradley Clement of Caltech for NASA's Jet Propulsion Laboratory. Further information is contained in a TSP (see page 1).

This software is available for commercial licensing. Please contact Don Hart of the California Institute of Technology at (818) 393-3425. Refer to NPO-30614.

Software Reduces Radio-Interference Effects in Radar Data

A computer program suppresses the effects of narrow-band radio-frequency interference (RFI) on the data collected by a wide-band radar system. The need for this program arises because some advanced wide-band synthetic-aperture radar systems utilize frequency bands that include frequencies used by other radio services. In this program, the RFI environment is represented by an autoregressive process, the frequency band of which is narrow relative to that of the radar. Most of the RFI signals, both narrow- and wide-band, are estimated in one pass of a least-mean-square (LMS)

adaptive filter. The program implements three popular LMS algorithms: the time-domain LMS, the frequency-domain LMS, and the filter-bank LMS adaptive-filter algorithms. The program can be run in a manual or automatic mode. In the manual mode, the user selects the filter parameters prior to execution. In the automatic mode, the program uti-

lizes median-filter and spectral-estimation techniques plus the variable-step-size LMS algorithm for automatic determination of filter parameters, and the parameters are adaptively changed as functions of the inputs, resulting in better overall performance.

This program was written by Charles T-C Le, Scott Hensley, and Elaine Chapin of Cal-

tech for NASA's Jet Propulsion Laboratory. Further information is contained in a TSP (see page 1).

This software is available for commercial licensing. Please contact Don Hart of the California Institute of Technology at (818) 393-3425. Refer to NPO-40255.



Using Iron To Treat Chlorohydrocarbon-Contaminated Soil

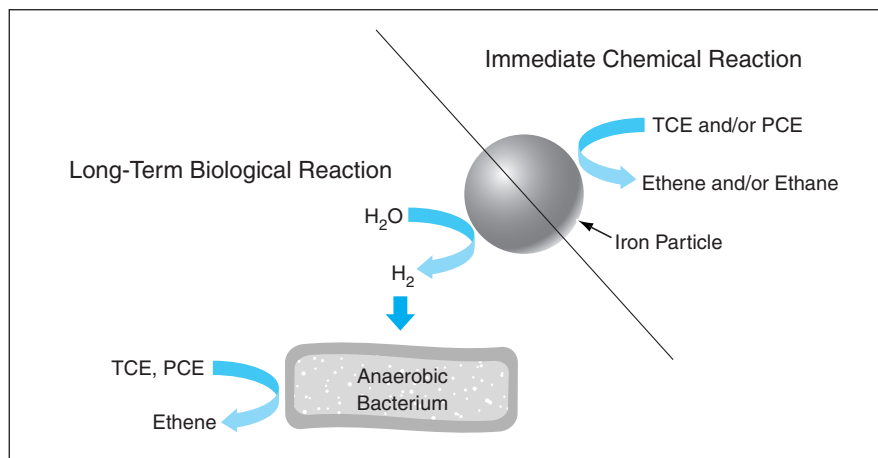
Prompt chemical remediation is followed by longer-term enhanced bioremediation.

John F. Kennedy Space Center, Florida

A method of *in situ* remediation of soil contaminated with chlorinated hydrocarbon solvents involves injection of nanometer-size iron particles. This method should not be confused with a similar method, involving injection of emulsified iron particles, reported in "Treatment To Destroy Chlorohydrocarbon Liquids in the Ground" (KSC-12246), *NASA Tech Briefs*, Vol. 27, No. 6 (June 2003), page 56. Like that method, this method is implemented in a process that is safe, yields environmentally benign end products, takes less time and costs less than do traditional pump-and-treat processes, and is both less expensive and less environmentally disruptive than are cleanup processes that involve excavation, transport to facilities for incineration or other treatment, and reburial in landfills.

In a related prior method of bioremediation of soil contaminated with trichloroethylene (TCE) or perchloroethylene (PCE), also known as tetrachloroethylene, electron donors and nutrients are supplied to contaminated soil so that anaerobic bacteria naturally present in the soil can use the electron donors in breaking down chlorohydrocarbon molecules in their metabolic pathways. In the metabolic process in question, denoted reductive dechlorination or dehalorespiration, one or more chlorine atom(s) are removed from each chlorinated hydrocarbon molecule and replaced with hydrogen atoms.

The present method exploits a combination of prompt chemical remediation followed by longer-term enhanced bioremediation (see figure) and, optionally, is practiced in conjunction with the method of bioremediation described above. Newly injected iron particles chemically reduce chlorinated hydrocarbons upon contact. Thereafter, in the presence of groundwater, the particles slowly corrode via chemical reactions that effect sustained release of dis-



An **Injected Iron Particle** causes the reduction of chlorinated hydrocarbons (especially TCE and PCE). These compounds are converted to hydrocarbons along two reaction pathways: an immediate chemical reduction and a long-term biological reduction.

solved hydrogen. The hydrogen serves as an electron donor, increasing the metabolic activity of the anaerobic bacteria and thereby sustaining bioremediation at a rate higher than the natural rate.

Wells for injecting the iron particles are installed in a contaminated site in locations such that the particles become entrained in the underground plume of groundwater and contaminants flowing from the site. The particles are small enough that they can be transported through compact soil and thereby become dispersed throughout a large volume.

The effects of choosing various locations for injection wells and of injecting various amounts of iron are assessed by a technique in which helium, used as a tracer gas, is injected into the ground via the wells. Helium was chosen as the tracer gas because of its low background concentration in the atmosphere, low rate of diffusion in water, moderate solubility in water, non-toxicity, chemical inertness, and the similarity of its physical characteristics to those of hydrogen. The decrease in the concentration of helium with distance from the point of

injection is taken as an approximate indication of the abiotic component of the loss of dissolved hydrogen; the difference between decrease in the concentration of hydrogen and that of helium is then taken as an approximate indication of the biotic component of the loss of dissolved hydrogen. Monitoring by use of this technique can provide information that helps to determine the minimum amount of iron that must be injected to remediate the contaminated site.

This work was done by G. Duncan Hitchens, Dalibor Hodko, Heekyung Kim, Tom Rogers, Waheguru Pal Singh, Anthony Giletto, and Alan Cisar of Lynntech, Inc., for Kennedy Space Center.

In accordance with Public Law 96-517, the contractor has elected to retain title to this invention. Inquiries concerning rights for its commercial use should be addressed to:

*Jinseong Kim
Lynntech, Inc.
7610 Eastmark Drive
College Station, TX 77840
E-mail: jinseong.kim@lynntech.com*

Refer to KSC-12299, volume and number of this NASA Tech Briefs issue, and the page number.



Thermally Insulating, Kinematic Tensioned-Fiber Suspension

Tensioned polymer fibers afford both rigidity and high thermal resistance.

Goddard Space Flight Center, Greenbelt, Maryland

Figure 1 shows a salt pill and some parts of a thermally insulating, kinematic suspension system that holds the salt pill rigidly in an adiabatic-demagnetization refrigerator (ADR). “Salt pill” in this context denotes a unit comprising a cylindrical container, a matrix of gold wires in the container, and a cylinder of ferric ammonium alum (a paramagnetic salt) that has been deposited on the wires. The structural members used in this system for both thermal insulation and positioning are

aromatic polyamide fibers (Kevlar® or equivalent) under tension.

This suspension system is designed to satisfy several special requirements to ensure the proper operation of the ADR. These requirements are to (1) maintain the salt pill at a specified position within the cylindrical bore of an electromagnet; (2) prevent vibrations, which would cause dissipation of heat in the salt pill; and (3) minimize the conduction of heat from the electromagnet bore and other neighboring objects to

the salt pill; all while (4) protecting the salt pill (which is fragile) against all tensile and bending loads other than those attributable to its own weight. In addition, the system is required to consist of two subsystems — one for the top end and one for the bottom end of the salt pill — that can be assembled and tensioned separately from each other and from the salt pill, then later attached to the salt pill.

The main reason for choosing aromatic polyamide fibers is that they exhibit a high ratio of stiffness to thermal conductivity in the cryogenic temperature range of the ADR. Their stiffness is about three times that of steel fibers of the same weight. To form each tension member, a bundle of the fibers is formed into a loop by gluing its ends together, the loop is doubled back upon itself several times, and the loop is strung between pulleys, which are then pulled apart by a spring-loading mechanism to place the fibers under tension.

The system is characterized as kinematic because the tension members are positioned and oriented to restrain the salt pill once (and only once) against motion in each of its six degrees of freedom. Figure 2 schematically depicts the overall kinematic configuration, omitting details of the kinematic configurations and spring-loading schemes within the two end suspension subsystems. The top suspension subsystem restrains the top end of the salt pill against translation in any direction (thereby eliminating three degrees of freedom) and against rotation about the cylindrical axis of the salt pill (thereby eliminating another degree of freedom). The bottom suspension subsystem restrains the bottom end of the salt pill against motion in any direction in the plane perpendicular to the cylindrical axis of the salt pill, thereby eliminating the remaining two degrees of freedom.

This work was done by George M. Voellmer of Goddard Space Flight Center. Further information is contained in a TSP (see page 1). GSC-14743-1

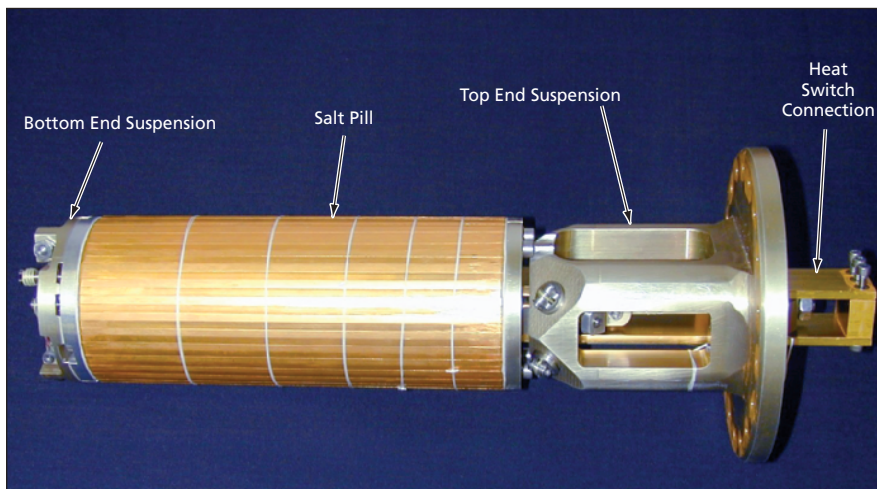


Figure 1. The Bottom and Top Suspension Subsystems contain tensioned, thermally insulating polymer fibers in kinematic arrangements. When the components shown here are mounted in the bore of an ADR electromagnet, the salt pill is held rigidly in the specified position.

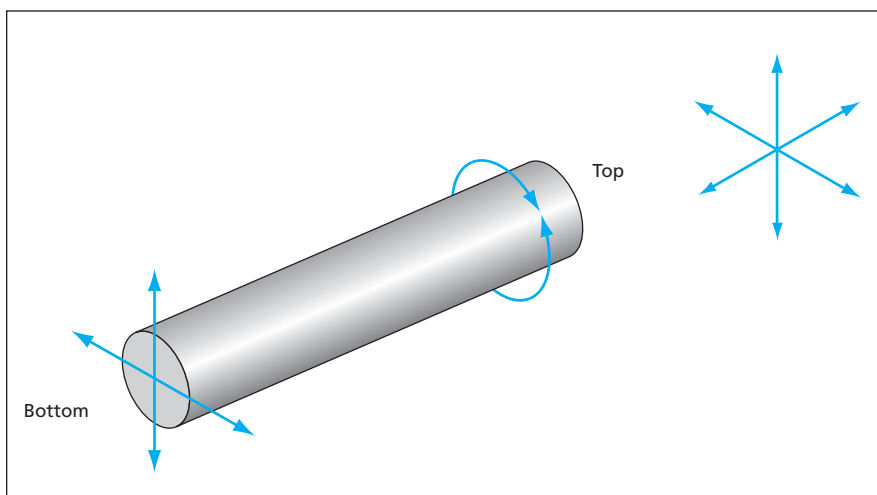


Figure 2. Motion of the Salt Pill in the degrees of freedom indicated by the arrows is prevented by the kinematic suspension system.

Back Actuators for Segmented Mirrors and Other Applications

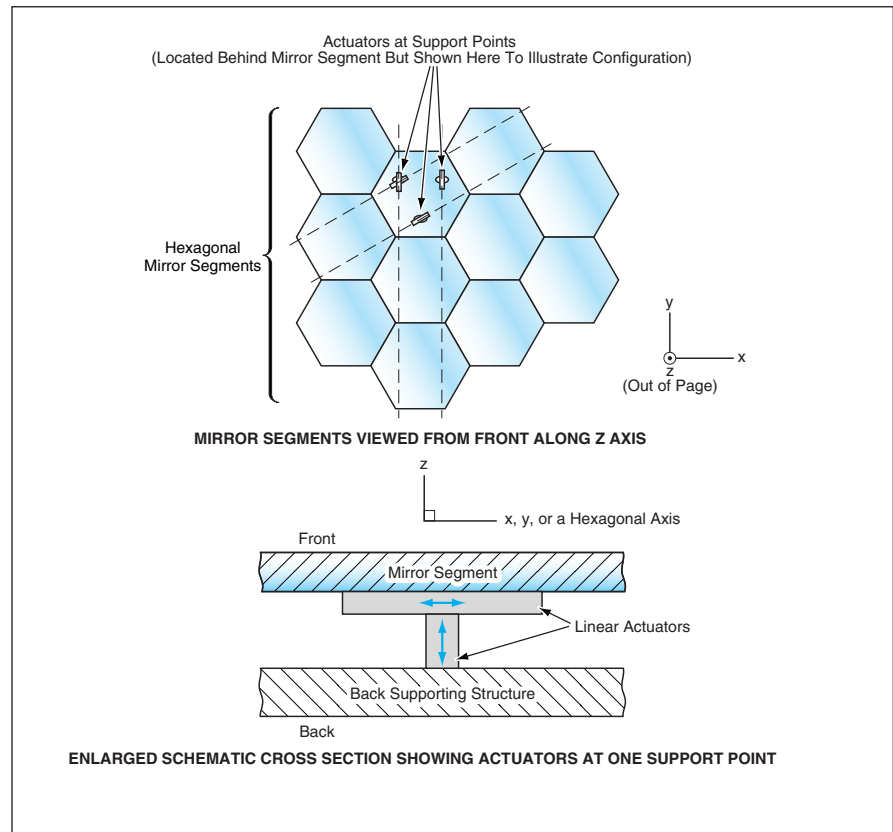
Actuation mechanisms could be simpler.

NASA's Jet Propulsion Laboratory, Pasadena, California

Back actuators have been proposed as alternatives to edge actuators considered previously for use in aligning hexagonal segments of lightweight segmented astronomical mirrors planned for use in outer space. The proposed back actuators could also be useful on Earth as parts of wafer-conveyance systems in the semiconductor industry.

Whereas the prior edge actuators were required to impose rotations and torques (in addition to forces and displacements) at joints between mirror segments, the proposed back actuators would be required to impose only forces and displacements (sometimes accompanied by small incidental torques and rotations). The advantages of the back-actuation approach, relative to the edge-actuation approach, are that the actuation mechanisms could be made simpler and a single overall actuation scheme could incorporate what were previously separate actuation schemes for (1) orienting the mirror segments at the required angles and (2) placing the mirror segments at the required distances along the optical axis from the focus.

Each hexagonal mirror segment would be supported at three points by sets of linear actuators (see figure). The linear actuators at each support point would include one to impose displacement along the optical axis (the z axis in the figure) plus one or two to impose displacement along one or two of the hexagonal axes. The linear actuators could be, for example,



Actuators would be located on the backs of hexagonal mirror segments instead of at the edges between mirror segments as before. The combination of linear displacements along the relevant coordinate axes at the three support points of each segment would suffice to align all of the mirror segments in both position and orientation.

shape-memory-alloy actuators or piezoelectric actuators that move in the manner of an inchworm like those described in several previous NASA Tech Briefs articles.

This work was done by Eui-Hyeok Yang and Dean Wiberg of Caltech for NASA's Jet Propulsion Laboratory. Further information is contained in a TSP (see page 1). NPO-30550

Mechanism for Self-Reacted Friction Stir Welding

This mechanism performs better than others that have been tried.

Marshall Space Flight Center, Alabama

A mechanism has been designed to apply the loads (the stirring and the resection forces and torques) in self-reacted friction stir welding. This mechanism differs somewhat from mechanisms used in conventional friction stir welding, as described below.

The tooling needed to apply the large reaction loads in conventional friction stir welding can be complex. Self-reacted

friction stir welding has become popular in the solid-state welding community as a means of reducing the complexity of tooling and to reduce costs. The main problems inherent in self-reacted friction stir welding originate in the high stresses encountered by the pin-and-shoulder assembly that produces the weld.

The design of the present mechanism solves the problems. The mechanism

(see figure) includes a redesigned pin-and-shoulder assembly. The welding torque is transmitted into the welding pin by a square pin that fits into a square bushing with setscrews. The opposite or back shoulder is held in place by a Woodruff key and high-strength nut on a threaded shaft. The Woodruff key reacts the torque, while the nut reacts the tensile load on the shaft.



This Mechanism Applies All the Loads needed for self-reacted friction stir welding.

The welding pin and shoulder can be assembled and disassembled quickly. An additional advantage of the present mechanism is that it affords positive seal-

ing on the root-side shoulder to reduce winking of the material being welded. This mechanism has been proven superior to all mechanisms tried before in

self-reacted friction stir welding.

This work was done by Richard Venable and Joseph Bucher of Lockheed Martin Corp. for Marshall Space Flight Center. For further information, contact Gary L. Wilett at (504) 257-4786.

Title to this invention has been waived under the provisions of the National Aeronautics and Space Act {42 U.S.C. 2457(f)} to Lockheed Martin Manned Space Systems. Inquiries concerning licenses for its commercial development should be addressed to:

*Lockheed Martin Manned Space Systems
P.O. Box 29304
New Orleans, LA 70189*

Refer to MFS-31914, volume and number of this NASA Tech Briefs issue, and the page number.



Lightweight Exoskeletons With Controllable Actuators

Resistive or assistive forces and torques would be generated on command.

NASA's Jet Propulsion Laboratory, Pasadena, California

A proposed class of lightweight exoskeletal electromechanical systems would include electrically controllable actuators that would generate torques and forces that, depending on specific applications, would resist and/or assist wearers' movements. The proposed systems would be successors to relatively heavy, bulky, and less capable human-strength-amplifying exoskeletal electromechanical systems that have been subjects of research during the past four decades. The proposed systems could be useful in diverse applications in which there are needs for systems that could be donned or doffed easily, that would exert little effect when idle, and that could be activated on demand: exam-

ples of such applications include (1) providing controlled movement and/or resistance to movement for physical exercise and (2) augmenting wearers' strengths in the performance of military, law-enforcement, and industrial tasks.

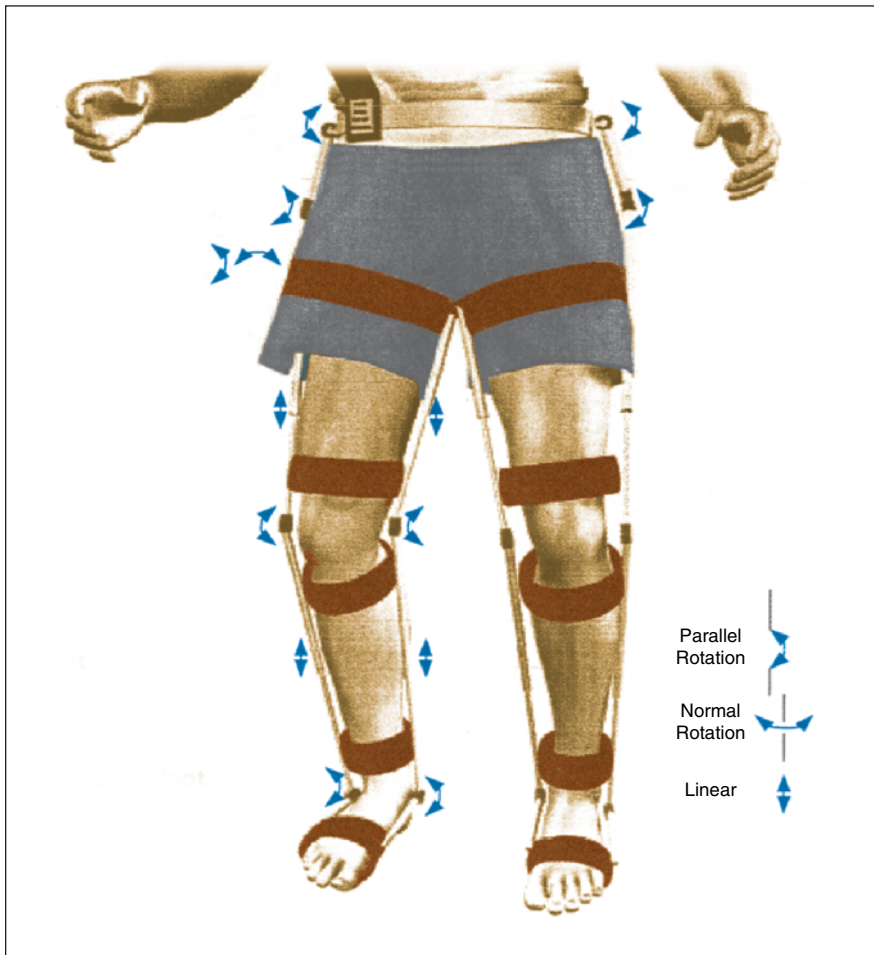
An exoskeleton according to the proposal would include adjustable lightweight graphite/epoxy struts and would be attached to the wearer's body by belts made of hook-and-pile material (see figure). At selected rotary and linear joints, the exoskeleton would be fitted, variously, with lightweight, low-power-consumption rotary and linear brakes, clutches, and motors. The exoskeleton would also be equipped with electronic circuitry for monitoring, control, and

possibly communication with external electronic circuits that would perform additional monitoring and control functions.

The linear motors could be lightweight actuators that move in the manner of an inchworm. The rotary motor actuators could be fairly conventional rotary motors, possibly equipped with clutches. Each brake or clutch would be, essentially, a rotary or linear dashpot of advanced design, containing an electrorheological fluid. (A typical electrorheological fluid is a dielectric fluid containing suspended microscopic dielectric particles. The viscosity of the fluid increases with applied electric field, with a typical response time of the order of milliseconds.) Within each brake or clutch, electrodes and flow channels would be sized, shaped, and placed so that in the absence of applied voltage, there would be minimal resistance to the affected linear or rotary motion, while at the maximum applied voltage, the actuator would resist the motion with a required force or torque, respectively. Because very little power is consumed in applying an electric field to an electrorheological liquid, a system according to the proposal used only for controlled-resistance exercise would consume little power and, hence, could be powered by a small, lightweight battery.

The electronic circuitry of the exoskeleton would include a Pentium (or equivalent) digital processor, digital-to-analog and analog-to-digital converter circuit boards, motion-control circuits, sensor-interface circuit boards, and a modem circuit card for radio communication with a remote control station. A small display device would present data on required and performed physical activity. Most of this circuitry could be mounted in a backpack.

Miniature position sensors would be placed on the joints of the exoskeleton. Miniature force and touch sensors and myoelectric or myopneumatic sensors would be placed on the wearer's body to measure flexion and extension of muscles. The sensor and control circuitry would be designed to act together to en-



An Exoskeleton could be attached to a whole human body or, as in this example, to part of the body to provide exercise or assistance in motions that involve selected joints.

able the wearer to act intuitively in controlling the exoskeleton. The software in the microprocessor would (1) take account of all sensor signals to infer the motion of, and the forces and torques exerted by and on, the wearer and (2)

generate commands to assist or resist the wearer's motion as needed. The sensor and control design would be characterized by redundancy and robustness.

This work was done by Yoseph Bar-Cohen, Constantinos Mavrodis, Juan Melli-Huber,

and Avi (Alan) Fisch of Caltech for NASA's Jet Propulsion Laboratory. Further information is contained in a TSP (see page 1). NPO-30558

⚙️ Miniature Robotic Submarine for Exploring Harsh Environments

Extreme miniaturization would enable exploration of previously inaccessible regions.

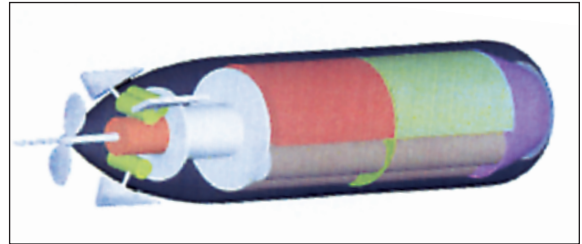
NASA's Jet Propulsion Laboratory, Pasadena, California

The miniature autonomous submersible explorer (MASE) has been proposed as a means of scientific exploration — especially, looking for signs of life — in harsh, relatively inaccessible underwater environments. Basically, the MASE would be a small instrumented robotic submarine (see figure) that could launch itself or could be launched from another vehicle. Examples of environments that might be explored by use of the MASE include subglacial lakes, deep-ocean hydrothermal vents, acidic or alkaline lakes, brine lenses in permafrost, and ocean regions under Antarctic ice shelves.

The instrumentation carried aboard the MASE would include one or more high-resolution video camera(s), circuitry for capturing image data from the

cameras, and microelectromechanical-systems-based (MEMS-based) sensors designed to gather scientific data under the extreme conditions (e.g., high pressure, high or low temperature, acidity or alkalinity) of the aqueous environment to be explored. The instrumentation would be contained in easily interchangeable modules. The MASE would be equipped for autonomous control, real-time processing of scientific data, and high-speed, full-duplex communication with a monitoring station via a fiber-optic tether.

The basic MASE concept allows for variations for different applications. In



The MASE would be 20 cm long and 5 cm in diameter — small enough to be carried aboard another vehicle prior and to explore confined spaces inaccessible to larger exploratory vehicles.

most applications now envisioned, the MASE would be designed as a disposable system to be used once.

This work was done by Alberto Behar, Fredrik Bruhn, and Frank Carsey of Caltech for NASA's Jet Propulsion Laboratory. Further information is contained in a TSP (see page 1). NPO-40501



Electron-Spin Filters Based on the Rashba Effect

Filters would be made from nonmagnetic semiconductors and operated without applied magnetic fields.

NASA's Jet Propulsion Laboratory, Pasadena, California

Semiconductor electron-spin filters of a proposed type would be based on the Rashba effect, which is described briefly below. Electron-spin filters — more precisely, sources of spin-polarized electron currents — have been sought for research on, and development of, the emerging technological discipline of spintronics (spin-based electronics). There have been a number of successful demonstrations of injection of spin-polarized electrons from diluted magnetic semiconductors and from ferromagnetic

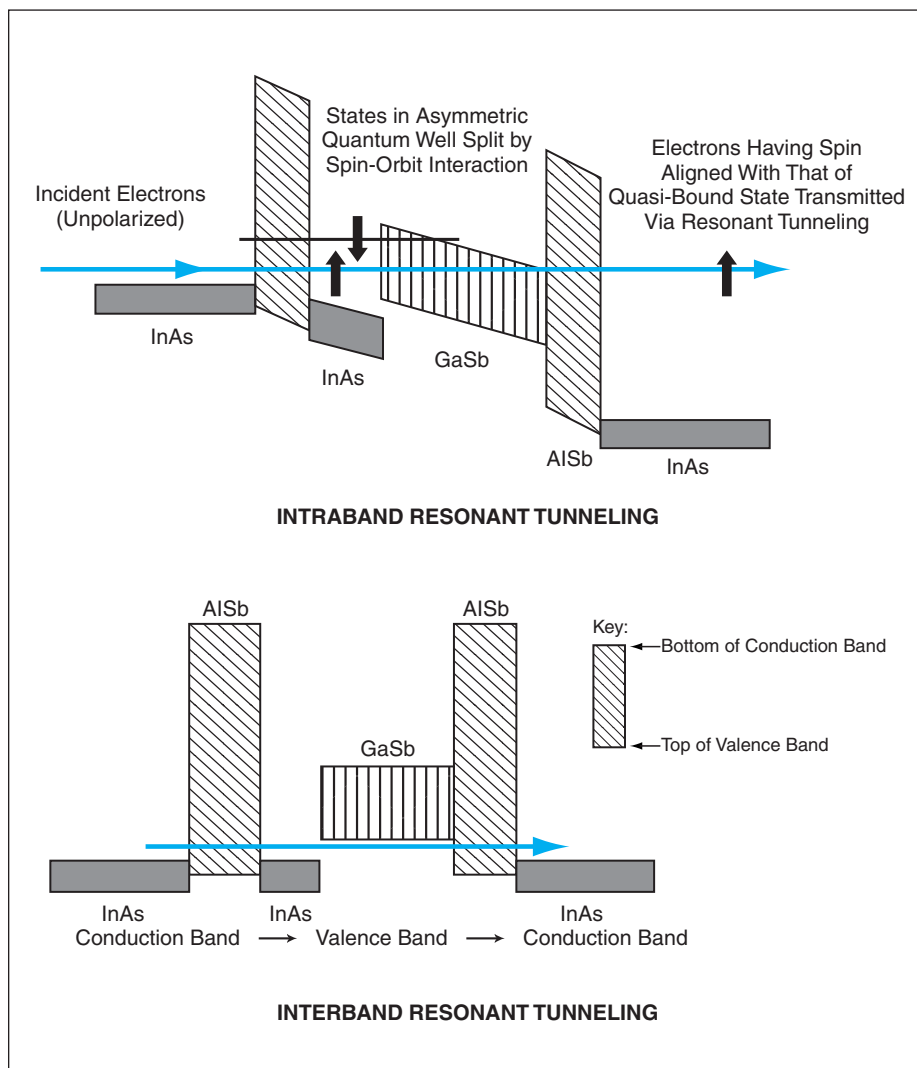
metals into nonmagnetic semiconductors. In contrast, a device according to the proposal would be made from nonmagnetic semiconductor materials and would function without an applied magnetic field.

The Rashba effect, named after one of its discoverers, is an energy splitting, of what would otherwise be degenerate quantum states, caused by a spin-orbit interaction in conjunction with a structural-inversion asymmetry in the presence of interfacial electric fields in a

semiconductor heterostructure. The magnitude of the energy split is proportional to the electron wave number. The present proposal evolved from recent theoretical studies that suggested the possibility of devices in which electron energy states would be split by the Rashba effect and spin-polarized currents would be extracted by resonant quantum-mechanical tunneling. Accordingly, a device according to the proposal would be denoted an asymmetric resonant interband tunneling diode [a-RITD]. An a-RITD could be implemented in a variety of forms, the form favored in the proposal being a double-barrier heterostructure containing an asymmetric quantum well.

It is envisioned that a-RITDs would be designed and fabricated in the InAs/GaSb/AlSb material system for several reasons: Heterostructures in this material system are strong candidates for pronounced Rashba spin splitting because InAs and GaSb exhibit large spin-orbit interactions and because both InAs and GaSb would be available for the construction of highly asymmetric quantum wells. This material system affords a variety of energy-band alignments that can be exploited to obtain resonant tunneling and other desired effects. The no-common-atom InAs/GaSb and InAs/AlSb interfaces would present opportunities for engineering interface potentials for optimizing Rashba spin splitting.

More specifically, a device of this type would comprise an asymmetric composite InAs-GaSb well, sandwiched between AlSb barriers and InAs electrodes. Unpolarized electrons from the conduction band of an InAs emitter electrode would tunnel rapidly through one AlSb barrier and through an asymmetric InAs-GaSb quantum well, where Rashba spin splitting would occur; they would then tunnel through the other AlSb barrier into the conduction band of an InAs collector electrode. With appropriately chosen



Electron-Energy-Band Alignments and two tunneling schemes of proposed InAs/GaSb/AlSb a-RITD devices are depicted here schematically. The shaded and cross-hatched regions represent bandgaps.

thicknesses of layers, this device could be made to operate in either of two regimes (see figure):

- Under low bias, in a resonant-interband-tunneling regime, in which electrons would traverse valence subband states in GaSb or
- Under moderate bias, in an intraband-resonant-tunneling regime, in which electrons would traverse conduction subband states in InAs. Computational simulations have led to an expectation

that the interband regime would yield better performance.

This work was done by David Z.-Y. Ting, Xavier Cartoixà, and Thomas C. McGill of Caltech; Jeong S. Moon, David H. Chow, and Joel N. Schulman of HRL Laboratories, LLC; and Darryl L. Smith of Los Alamos National Laboratory for NASA's Jet Propulsion Laboratory. Further information is contained in a TSP (see page 1).

In accordance with Public Law 96-517, the contractor has elected to retain title to this

invention. Inquiries concerning rights for its commercial use should be addressed to:

*Innovative Technology Assets Management
JPL*

*Mail Stop 202-233
4800 Oak Grove Drive
Pasadena, CA 91109-8099
(818) 354-2240*

*E-mail: iaoffice@jpl.nasa.gov
Refer to NPO-30635, volume and number of this NASA Tech Briefs issue, and the page number.*

Diffusion-Cooled Tantalum Hot-Electron Bolometer Mixers

Lower TCs should translate to lower noise and lower required local-oscillator power.

NASA's Jet Propulsion Laboratory, Pasadena, California

A batch of experimental diffusion-cooled hot-electron bolometers (HEBs), suitable for use as mixers having input frequencies in the terahertz range and output frequencies up to about a gigahertz, exploit the superconducting/normal-conducting transition in a thin strip of tantalum. The design and operation of these HEB mixers are based on mostly the same principles as those of a prior HEB mixer that exploited the superconducting/normal-conducting transition in a thin strip of niobium and that was described in "Diffusion-Cooled Hot-Electron Bolometer Mixer" (NPO-19719), *NASA Tech Briefs*, Vol. 21, No. 1 (January 1997), page 12a.

One reason for now choosing tantalum instead of niobium arises from the fact that the superconducting-transition

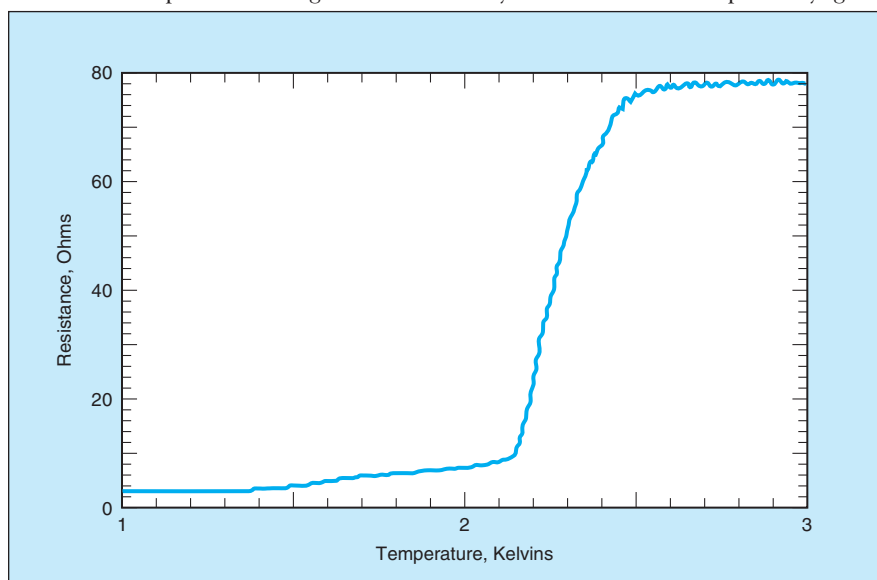
temperature (T_C) of tantalum lies between 2 and 3 K, while that of niobium lies between 6 and 7 K. Theoretically, the input mixer noise of a superconducting HEB is proportional to T_C and the power demand on the local oscillator that supplies one of the input signals to the mixer is proportional to T_C^2 . The lower noise and power demand associated with the lower T_C of tantalum could make tantalum HEBs more attractive, relative to niobium HEBs, in applications in which there are requirements to minimize noise and/or to provide mixers that can function well using the weak signals generated by typical solid-state local oscillators. Of course, to reach the required lower T_C , it is necessary to use more complex cryogenic

equipment. Fortunately, such equipment (e.g., helium-3 cryostats) is commercially available.

In order to make a practical tantalum HEB, it is necessary to overcome a challenge posed by the fact that thin films of tantalum tend to contain grains of two different crystalline phases. The presence of the two phases would be unacceptable in a practical device because (1) the additional electron scattering at the grain boundaries would tend to suppress the diffusion-cooling mechanism, and (2) the different T_C s of the two phases would lead to broadening of the transition.

The present HEB mixers contain tantalum microbridges having lengths of 100 to 400 nm, widths of 100 to 200 nm, and thicknesses of 10 nm. The bridges were made from a 10-nm-thick film of tantalum deposited by sputtering onto a 1.5-nm-thick seed layer of niobium on a silicon wafer. The niobium seed layer was used to promote the growth of one of the two crystalline phases (the α phase) to ensure the required crystalline purity and thereby keep the superconducting transition (see figure) as sharp as possible.

The results of microwave impedance tests of one of the experimental tantalum HEBs have been interpreted as signifying that the 3-dB roll-off frequency for mixer conversion efficiency can be expected to be about 1 GHz, neglecting the effect of electrothermal feedback. End effects are small enough (as illustrated by the smallness of the "foot" of the resistance-versus-temperature curve in the figure) that it should be possible to use devices as short as 100 nm and possibly even shorter. Inas-



DC Resistance of an HEB was measured as a function of temperature from below to above T_C . Except for the lower T_C , this plot is similar to the resistance-vs.-temperature plots of niobium HEBs. The nonzero-resistance "foot" of this plot is an effect of normally conductive gold contact pads at the ends of the device.

much as the thermal-relaxation time for diffusion cooling is proportional to the square of the device length, the 100-nm-long devices should be capable of “raw” speeds of about 16 GHz. Since only a few gigahertz of bandwidth is

needed for most mixer applications, it is expected that tantalum HEBs will be fast enough even in the presence of slowing effects of electrothermal feedback, which is present in most bolometer mixer circuits.

This work was done by Anders Skalare, William McGrath, Bruce Bumble, and Henry LeDuc of Caltech for NASA’s Jet Propulsion Laboratory. Further information is contained in a TSP (see page 1). NPO-30695

Tunable Optical True-Time Delay Devices Would Exploit EIT

Adjustable delays up to milliseconds would be generated within small volumes.

NASA’s Jet Propulsion Laboratory, Pasadena, California

Tunable optical true-time delay devices that would exploit electromagnetically induced transparency (EIT) have been proposed. Relative to prior true-time delay devices (for example, devices based on ferroelectric and ferromagnetic materials) and electronically controlled phase shifters, the proposed devices would offer much greater bandwidths. In a typical envisioned application, an optical pulse would be modulated with an ultra-wideband radio-frequency (RF) signal that would convey the information that one seeks to communicate, and it would be required to couple differently delayed replicas of the RF signal to the radiating elements of a phased-array antenna. One or more of the proposed devices would be used to impose the delays and/or generate the delayed replicas of the RF-modulated optical pulse. The beam radiated or received by the antenna would be steered by use of a microprocessor-based control system that would adjust operational parameters of the devices to tune the delays to the required values.

EIT is a nonlinear quantum optical interference effect that enables the propagation of light through an initially opaque medium. A suitable medium must have, among other properties, three quantum states (see Figure 1): an excited state (state 3), an upper ground state (state 2), and a lower ground state (state 1). These three states must form a closed system that exhibits no decays to other states in the presence of either or both of two laser beams: (1) a probe beam having the wavelength corresponding to the photon energy equal to the energy difference between states 3 and 1; and (2) a coupling beam having the wavelength corresponding to the photon energy equal to the energy difference between states 3 and 2. The probe beam is the one that is pulsed and modulated with an RF signal.

If a properly adjusted probe pulse is sent into the medium in the absence of the cou-

pling beam, the atoms completely absorb the pulse and jump from state 1 to state 3. This absorption is what makes the medium opaque. In the presence of the coupling beam, states 2 and 3 become coupled, preventing the absorption of the probe beam and thereby rendering the medium transparent to the probe beam. At resonance (that is, when the laser wavelengths correspond exactly to the differences between the energy levels of the quantum states of the medium), the index of refraction of the medium is exactly 1. At slightly different frequencies, the degree of cancellation of absorption of the probe beam is less and the index of refraction differs. The nature of the variation of the slope of the index of refraction as a function of wavelength is such as to substantially reduce the group velocity of a probe light pulse.

The reduction in group velocity can be exploited to slow and even stop the pulse. If the coupling pulse is turned off when the probe pulse reaches the middle of the medium, the probe pulse becomes trapped in the quantum states of the medium. The ratio between the numbers of atoms in states 1 and 2 is a measure of the ratio between the electric-field strengths of the probe and the coupling beams immediately before turn off. Also, the quantum state of the RF modulation of a stopped light pulse is stored in the spin quantum state of the medium. After a desired delay, the quantum state of the medium can be interrogated optically: Turning the coupling beam back on causes the regeneration of the optical pulse, complete with the RF modulation.

Suitably prepared clouds of alkali atoms (e.g., clouds of optically cooled sodium vapor) have been observed to exhibit EIT and would be used as the initially opaque media in the proposed devices. Recent experiments in compact cells (<1 cm³) of alkali-atom vapors have demonstrated that light pulses can be effectively decelerated to speeds of tens of meters per second and even stopped for controlled amounts of

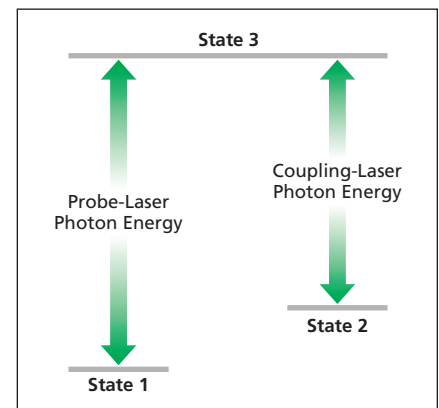


Figure 1. A Closed System of Three Quantum States that are accessible via laser beams is among characteristics essential for electromagnetically induced transparency.

time that can range from microseconds to milliseconds. In contrast, to obtain millisecond delays by use of optical fibers, it would be necessary to make the fibers hundreds of kilometers long, and the delays would not be adjustable because the lengths would not be adjustable.

A simple example of a device according to the proposal is depicted schematically in Figure 2. A probe laser beam would be split into two parts: an undelayed (reference) beam and a beam to be delayed. A single probe pulse would be generated, yielding a single reference pulse. The probe pulse would be trapped in the medium, then released by use of suitably timed coupling pulses. If the coupling pulses were cycled on and off several times with sufficient rapidity while the probe pulse was still inside the medium, then several differently delayed replicas of the probe pulse would be generated.

This work was done by Igor Kulikov, Leo DiDomenico, and Hwang Lee of Caltech for NASA’s Jet Propulsion Laboratory. Further information is contained in a TSP (see page 1). NPO-30776



Fast Query-Optimized Kernel-Machine Classification

Computation is accelerated by an order of magnitude, without loss of accuracy.

NASA's Jet Propulsion Laboratory, Pasadena, California

A recently developed algorithm performs kernel-machine classification via incremental approximate nearest support vectors. The algorithm implements support-vector machines (SVMs) at speeds 10 to 100 times those attainable by use of conventional SVM algorithms. The algorithm offers potential benefits for classification of images, recognition of speech, recognition of handwriting, and diverse other applications in which there are requirements to discern patterns in large sets of data.

SVMs constitute a subset of kernel machines (KMs), which have become popular as models for machine learning and, more specifically, for automated classification of input data on the basis of labeled training data. While similar in many ways to k -nearest-neighbors (k -NN) models and artificial neural networks (ANNs), SVMs tend to be more accurate. Using representations that scale only linearly in the numbers of training examples, while exploring nonlinear (kernelized) feature spaces that are exponentially larger than the original input dimensionality, KMs elegantly and practically overcome the classic "curse of dimensionality." However, the price that one must pay for the power of KMs is

that query-time complexity scales linearly with the number of training examples, making KMs often orders of magnitude more computationally expensive than are ANNs, decision trees, and other popular machine learning alternatives.

The present algorithm treats an SVM classifier as a special form of a k -NN. The algorithm is based partly on an empirical observation that one can often achieve the same classification as that of an exact KM by using only small fraction of the nearest support vectors (SVs) of a query.

The exact KM output is a weighted sum over the kernel values between the query and the SVs. In this algorithm, the KM output is approximated with a k -NN classifier, the output of which is a weighted sum only over the kernel values involving k selected SVs. Before query time, there are gathered statistics about how misleading the output of the k -NN model can be, relative to the outputs of the exact KM for a representative set of examples, for each possible k from 1 to the total number of SVs. From these statistics, there are derived upper and lower thresholds for each step k . These thresholds identify output levels for which the particular variant of the k -NN model already leans so strongly posi-

tively or negatively that a reversal in sign is unlikely, given the weaker SV neighbors still remaining.

At query time, the partial output of each query is incrementally updated, stopping as soon as it exceeds the predetermined statistical thresholds of the current step. For an easy query, stopping can occur as early as step $k = 1$. For more difficult queries, stopping might not occur until nearly all SVs are touched. A key empirical observation is that this approach can tolerate very approximate nearest-neighbor orderings. In experiments, SVs and queries were projected to a subspace comprising the top few principal-component dimensions and neighbor orderings were computed in that subspace. This approach ensured that the overhead of the nearest-neighbor computations was insignificant, relative to that of the exact KM computation.

This work was done by Dominic Mazzoni and Dennis DeCoste of Caltech for NASA's jet Propulsion Laboratory. Further information is contained in a TSP (see page 1).

The software used in this innovation is available for commercial licensing. Please contact Don Hart of the California Institute of Technology at (818) 393-3425. Refer to NPO-40441.

Indented Parts List Maintenance and Part Assembly Capture Tool — IMPACT

Viewing and maintaining the complex assembly hierarchies of large databases is made easier.

Lyndon B. Johnson Space Center, Houston, Texas

Johnson Space Center's (JSC's) indented parts list (IPL) maintenance and parts assembly capture tool (IMPACT) is an easy-to-use graphical interface for viewing and maintaining the complex assembly hierarchies of large databases. IMPACT, already in use at JSC to support the International Space Station (ISS), queries, updates, modifies, and views data in IPL and associated resource data, functions that it can also perform, with modification, for any large commercial database. By enabling its users to effi-

ciently view and manipulate IPL hierarchical data, IMPACT performs a function unlike that of any other tool. Through IMPACT, users will achieve results quickly, efficiently, and cost effectively.

Speed, efficiency, and cost are critical issues in maintaining complex assembly hierarchies of large databases. IPLs consist of parts organized into such complex assembly hierarchies. The more complex the hierarchy, the more the associated list grows and the more difficult it

becomes to locate a part to modify it. At JSC it was found that existing IPL manipulation methods were too complex, hard to use, and error-prone for time- and cost-sensitive ISS operations. IMPACT was therefore developed to address these drawbacks and to help users achieve results.

IMPACT uses a C++, X-Windows, and Motif application framework. At JSC, it operates with a PRO*C++ interface to an Oracle database. In this way, IMPACT can manipulate the vehicle master data-

base IPL with PL/SQL packages. Since it was developed using object-oriented programming in a modular fashion, it has proved easy to maintain and its capabilities are as easily extended. IMPACT has shown a very high reliability factor as well.

IMPACT manages a rapidly changing flight sequence, manifests, and detailed parts list for ISS by featuring views of an ISS IPL based on flight phases (i.e., launch, on-orbit, and return) and flights. It also features resource data viewing for each part in the IPL and a hypertext-based help system. IMPACT can be started in "view only" as well as in "update modes." When in update mode, IMPACT supports the creation of data-

base entries for new flights, elements, subelements, and parts as well as parts movement around assembly hierarchies, using menu-driven commands and buttons, and drag-and-drop technology. More than one IMPACT session can be brought up independent of another, and different views can be placed side-by-side on the same screen during the same session.

IMPACT is therefore a unique, flexible tool with an easy-to-use, highly intuitive graphical user interface. Its novelty lies in the fact that it allows users to view and manipulate IPL hierarchical data efficiently, something no other tool has allowed during the time of this reporting. Already in use on the ISS, IMPACT has

proven to be flexible and can mature and grow with a system. As such, it is a valuable adjunct not only to the space industry for which it was developed but, with suitable modifications, to large commercial databases.

This work was done by Bobby Jain, Bill Morris, and Kelly Sharpe of Barrios Technology for Johnson Space Center. For further information, contact

*Barrios Technology, Inc.
2525 Bay Area Blvd., Suite 300
Houston, TX 77058-1556
Phone: (281) 280-1900
Fax: (281) 280-1901*

Refer to MSC 22915, volume and number of this NASA Tech Briefs issue, and the page number.

➤ An Architecture for Controlling Multiple Robots

Hierarchies of behaviors can be constructed and coordinated with great versatility.

NASA's Jet Propulsion Laboratory, Pasadena, California

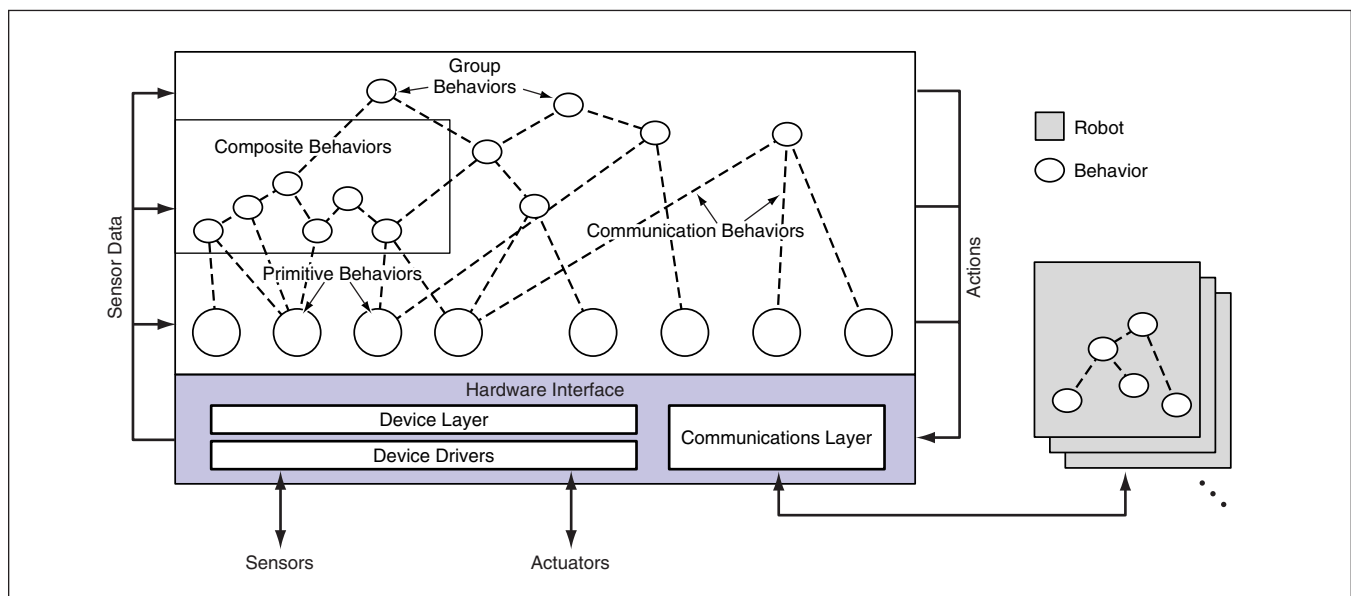
The Control Architecture for Multirobot Outpost (CAMPOUT) is a distributed-control architecture for coordinating the activities of multiple robots. In the CAMPOUT, multiple-agent activities and sensor-based controls are derived as group compositions and involve coordination of more basic controllers denoted, for present purposes, as behaviors.

The CAMPOUT provides basic mechanistic concepts for representation and execution of distributed group activities. One considers a network of nodes that com-

prise behaviors (self-contained controllers) augmented with hyper-links, which are used to exchange information between the nodes to achieve coordinated activities. Group behavior is guided by a scripted plan, which encodes a conditional sequence of single-agent activities. Thus, higher-level functionality is composed by coordination of more basic behaviors under the downward task decomposition of a multi-agent planner (see figure).

Robotics is a highly multidisciplinary field that requires efficient integration of

many components (e.g., perception, mapping, localization, control, and learning) that involve diverse representations, frameworks, and paradigms (e.g., classical control theory, artificially intelligent planners, estimation theory, data fusion, computer vision, utility theory, decision theory, fuzzy logic, and multiple-objective decision making). The CAMPOUT provides a conceptual infrastructure for consolidating diverse techniques to enable the efficient use and integration of these components for meaningful interaction and operation.



The CAMPOUT Provides for a Hierarchical Organization of primitive behaviors, composite behaviors built from primitive behaviors, and groups composed from coordination of behaviors across multiple robots. Each robot runs an instance of this architecture and participates in coordination of activities through group behaviors. Coordination is facilitated through communication behaviors.

The methodology of the CAMPOUT features a few elementary architectural mechanisms for (a) behavior representation, (b) behavior composition, (c) group coordination of teams, and (d) interfaces among (a), (b), and (c). For the purposes of the CAMPOUT, a behavior is defined and represented as a mapping from a percept (defined here as a description of raw or processed sensory input) or a sequence of percepts to an action or sequence of actions. The mapping assigns, to each possible action, a degree of preference that ranges from 0 for most undesired to 1 for most desired. This definition of a behavior is a general recipe that does not dictate how the mapping is to be implemented. It does not exclude implementation by use of a look-up table, a finite-state machine, a neural network, an expert system, a control law, or any other such means. Each behavior can be implemented using whichever approach is appropriate.

Behavior composition is the mechanism used for building higher-level behaviors by combining lower-level ones. The activities of lower-level behaviors are coordinated within the context of the task and

objective of a higher-level behavior. An explicit design goal of the CAMPOUT has been to support not one but an arbitrary number of behavior-coordination mechanisms (BCMs). The architecture can be extended by incorporation of new BCMs. Because different BCMs often require different behavior representations, the CAMPOUT involves utilization of a multi-valued behavior representation that is general enough for a large class of applications. BCMs can be divided into two main classes: arbitration and command. The CAMPOUT supports both classes.

In the CAMPOUT, the problem of coordinating a group of robots is formulated as one of coordinating multiple distributed behaviors across a network that includes more than one decision maker. In behavior coordination, one is basically concerned with resolving or managing conflicts between mutually exclusive alternatives and between behavioral objectives. Because this is as true for individual as for group decision-making, the difference between individual and group decision-making is inessential, and both can be studied in the same

conceptual framework. Mechanisms that are typically used for coordination of the behavior of one robot can then be used for coordination of behaviors running on a network of robots. Hence, for example, a control loop could use sensors on one robot to drive a different robot.

This work was done by Hrand Aghazarian, Paolo Pirjanian, Paul Schenker, and Terrance Huntsberger of Caltech for NASA's Jet Propulsion Laboratory. Further information is contained in a TSP (see page 1).

In accordance with Public Law 96-517, the contractor has elected to retain title to this invention. Inquiries concerning rights for its commercial use should be addressed to:

*Innovative Technology Assets Management
JPL*

*Mail Stop 202-233
4800 Oak Grove Drive
Pasadena, CA 91109-8099
(818) 354-2240*

E-mail: iaoffice@jpl.nasa.gov

Refer to NPO-30345, volume and number of this NASA Tech Briefs issue, and the page number.



Progress in Fabrication of Rocket Combustion Chambers by VPS

Several documents in a collection describe aspects of the development of advanced materials and fabrication processes intended to enable the manufacture of advanced rocket combustion chambers and nozzles at relatively low cost. One concept discussed in most of the documents is the fabrication of combustion-chamber liners by vacuum plasma spraying (VPS) of an alloy of 88Cu/8Cr/4Nb (numbers indicate atomic percentages) — a concept that was reported in “Improved Alloy for Fabrication of Combustion Chambers by VPS” (MFS-26546), *NASA Tech Briefs*, Vol. 23, No. 1 (January 1999), page 50. Another concept is the deposition of graded-composition wall and liner structures by VPS in order to make liners integral parts of wall structures and to make oxidation- and thermal-protection layers integral parts of liners: The VPS process is started at 100 percent of a first alloy, then the proportion of a second alloy is increased gradually from zero as deposition continues, ending at 100 percent of the second alloy. Yet another concept discussed in one of the documents is the VPS of oxidation-protection coats in the forms of nickel-and-chromium-containing refractory alloys on VPS-deposited 88Cu/8Cr/4Nb liners.

This work was done by Richard R. Holmes of Marshall Space Flight Center and Timothy N. McKechnie of Plasma Processes.

This invention is owned by NASA, and a patent application has been filed. For further information, contact Sammy Nabors, MSFC Commercialization Assistance Lead, at sammy.a.nabors@nasa.gov. Refer to MFS-31267.

CHEM-Based Self-Deploying Spacecraft Radar Antennas

A document proposes self-deploying spacecraft radar antennas based on cold hibernated elastic memory (CHEM) structures. Described in a number of prior *NASA Tech Briefs* articles, the CHEM concept is one of utilizing open-cell shape-memory-polymer (SMP) foams to make lightweight structures that can be compressed for storage and can later be expanded, then rigidified for use. A CHEM-based antenna according to the

proposal would comprise three layers of microstrip patches and transmission lines interspersed with two flat layers of SMP foam, which would serve as both dielectric spacers and as means of deployment. The SMP foam layers would be fabricated at full size at a temperature below the SMP glass-transition temperature (T_g). The layers would be assembled into a unitary structure, which, at temperature above T_g , would be compacted to much smaller thickness, then rolled up for storage. Next, the structure would be cooled to below T_g and kept there during launch. Upon reaching the assigned position in outer space, the structure would be heated above T_g to make it rebound to its original size and shape. The structure as thus deployed would then be rigidified by natural cooling to below T_g .

This work was done by Witold Sokolowski, John Huang, and Reza Ghaffarian of Caltech for NASA's Jet Propulsion Laboratory. Further information is contained in a TSP (see page 1). NPO-30742

Scalable Multiprocessor for High-Speed Computing in Space

A report discusses the continuing development of a scalable multiprocessor computing system for hard real-time applications aboard a spacecraft. “Hard real-time applications” signifies applications, like real-time radar signal processing, in which the data to be processed are generated at “hundreds” of pulses per second, each pulse “requiring” millions of arithmetic operations. In these applications, the digital processors must be tightly integrated with analog instrumentation (e.g., radar equipment), and data input/output must be synchronized with analog instrumentation, controlled to within fractions of a microsecond. The scalable multiprocessor is a cluster of identical commercial-off-the-shelf generic DSP (digital-signal-processing) computers plus generic interface circuits, including analog-to-digital converters, all controlled by software. The processors are computers interconnected by high-speed serial links. Performance can be increased by adding hardware modules and correspondingly modifying the software. Work is distributed among the processors in a parallel or pipeline fashion by means of a flexible master/slave control and timing

scheme. Each processor operates under its own local clock; synchronization is achieved by broadcasting master time signals to all the processors, which compute offsets between the master clock and their local clocks.

This work was done by James Lux, Minh Lang, Kouji Nishimoto, Douglas Clark, Dorothy Stosic, Alex Bachmann, William Wilkinson, and Richard Steffke of Caltech for NASA's Jet Propulsion Laboratory. Further information is contained in a TSP (see page 1).

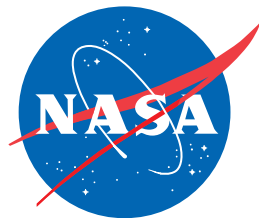
The software used in this innovation is available for commercial licensing. Please contact Don Hart of the California Institute of Technology at (818) 393-3425. Refer to NPO-40270.

Simple Systems for Detecting Spacecraft Meteoroid Punctures

A report describes proposed systems to be installed in spacecraft to detect punctures by impinging meteoroids or debris. Relative to other systems that have been used for this purpose, the proposed systems would be simpler and more adaptable, and would demand less of astronauts' attention and of spacecraft power and computing resources. The proposed systems would include a thin, hollow, hermetically sealed panel containing an inert fluid at a pressure above the spacecraft cabin pressure. A transducer would monitor the pressure in the panel. It is assumed that an impinging object that punctures the cabin at the location of the panel would also puncture the panel. Because the volume of the panel would be much smaller than that of the cabin, the panel would lose its elevated pressure much faster than the cabin would lose its lower pressure. The transducer would convert the rapid pressure drop to an electrical signal that could trigger an alarm. Hence, the system would provide an immediate indication of the approximate location of a small impact leak, possibly in time to take corrective action before a large loss of cabin pressure could occur.

This work was done by Stephen B. Hall of Marshall Space Flight Center. Further information is contained in a TSP (see page 1).

This invention is owned by NASA, and a patent application has been filed. For further information, contact Sammy Nabors, MSFC Commercialization Assistance Lead, at (256) 544-5226 or sammy.a.nabors@nasa.gov. Refer to MFS-31636.



National Aeronautics and
Space Administration